narra TX

**Review Article**

# Novel antibiotics, antifungals, antivirals, and anticancer agents from microbial sources (2023–2026): Chemistry, biosynthesis, and therapeutic potential

**Andri Frediansyah[1*], Fida L. Azzahra[2], Siriwan Kantisin[3,4], Keshab Bhattarai[5], Abrory AC. Pramana[6,7], Ni P. Ariantari[8] and Donna M. Ariestanti[9]**

[1]Research Center for Food Technology and Processing, National Research and Innovation Agency (BRIN), Yogyakarta, Indonesia; [2]Department of Chemistry, Faculty of Science, Chulalongkorn University, Bangkok, Thailand; [3]Department of Occupational Health and Safety, School of Health Science, Mae Fah Luang University, Chiang Rai, Thailand; [4]Area-Based Research and Innovation in Cross-Border Health Care Group, Mae Fah Luang University, Chiang Rai, Thailand; [5]Biofunctional Metabolites and Structures, Forschungszentrum Borstel, Leibniz Lungenzentrum, Germany; [6]Department of Biochemistry, Faculty of Medicine, Nursing, and Public Health, University of Gadjah Mada, Sleman, Indonesia; [7]Division of Nutritional Sciences, College of Agricultural, Agricultural, Consumer and Environmental Sciences, University of Illinois Urbana-Champaign, United States of America; [8]Department of Pharmacy, Faculty of Mathematics and Natural Sciences, Udayana University, Badung, Indonesia; [9]Faculty of Pharmacy, Universitas Indonesia, Depok, Indonesia

*Corresponding author: andri.frediansyah@brin.go.id

## Abstract

The growing burden of antimicrobial resistance, emerging viral infections, invasive fungal diseases, and cancer continues to create an urgent demand for new therapeutic agents with novel chemical scaffolds and mechanisms of action. Microbial natural products remain an important source of drug leads; however, many biosynthetic gene clusters remain silent or underexplored, and recent advances in genome mining, synthetic biology, metabolomics, and artificial intelligence have generated a rapidly expanding body of discoveries that requires integrated synthesis. This review summarizes and critically discusses recent advances in microbial-derived antibiotics, antifungals, antivirals, and anticancer agents reported from 2023 to 2026, with emphasis on their chemistry, biosynthesis, biological activities, and therapeutic potential. The review highlights major discovery platforms, including genome mining, heterologous expression, metabolomics-guided dereplication, molecular networking, and artificial intelligence-assisted biosynthetic prediction. It also discusses key biosynthetic classes, including ribosomally synthesized and post-translationally modified peptides, nonribosomal peptides, nonribosomal peptide–polyketide hybrids, polyketides, terpenoids, siderophores, metallophores, cyanobacterial metabolites, marine-derived compounds, and fungal natural products. In addition, this review explores the therapeutic relevance of microbial metabolites against bacterial, fungal, viral, and cancer targets, while considering translational challenges such as bioavailability, toxicity, resistance, production yield, and in vivo efficacy. Overall, the review emphasizes the continuing importance of microbial natural products as a chemically diverse and mechanistically innovative resource for future drug discovery.

**Keywords:** Genome mining, lasso peptides, terpenes, antimicrobial resistance, anticancer natural compounds

## Introduction

Natural products remain a major source of medicines, with >60% of approved small-molecule drugs having a natural origin [1,2]. Microbial secondary metabolites have revolutionized human



**Received: May 2, 2026 - Accepted: July 28, 2026 - Published online: July 31, 2026**

medicine, including penicillin, streptomycin, vancomycin, and doxorubicin. However, the pharmaceutical industry reduced investment in natural products in the late 20th century because of high rediscovery rates [2].

In the past decade, research on natural products has seen a spectacular renaissance made possible by new technologies. The explosion in microbial genome sequencing has revealed that even well-studied organisms possess a far greater biosynthetic potential than is expressed under standard laboratory conditions, with most biosynthetic gene clusters (BGCs) being silent [3,4]. At the same time, synthetic biology has provided powerful tools to activate these silent BGCs through promoter engineering, overexpression of regulators, and heterologous expression in optimized chassis strains [4,5]. For example, deletion of the global regulator wblA in *Streptomyces ghanaensis* activated a silent 92 kb BGC to produce the calcium-dependent lipopeptide olikomycin A [6], while promoter engineering derepressed the *bif* BGC for biffamycin A production [7]. Recent developments in metabolomics have enabled extensive profiling of microbial extracts and the use of molecular networking platforms to facilitate identification of novel compounds in complex mixtures [8,9]. Most recently, artificial intelligence has begun to revolutionize BGC prediction, substrate specificity determination, and even structure elucidation [10,11].

The period 2023–2026 is a critical juncture in this renaissance. Together, these emerging technologies now allow the systematic exploration of the biosynthetic potential encoded in microbial genomes. This work has resulted in the isolation of compounds with new chemical scaffolds, novel mechanisms of action, and significant therapeutic potential. The current review summarizes the key advances made during these three years, with an emphasis on the chemical diversity uncovered and biosynthetic principles revealed. Compounds are organized by biosynthetic class, encompassing RiPPs (lasso peptides, lanthipeptides, graspetides, sactipeptides), NRPS products and hybrids, polyketides, terpenoids, siderophores and metallophores, cyanobacterial metabolites, marine-derived compounds, and fungal natural products.

Genome mining has evolved from simple BGC identification to sophisticated platforms that can predict product architecture, select novel clusters, and allow experimental characterization. Version 7.0 of antiSMASH was released in 2023, with improved algorithms for BGC detection, cluster family analysis, and integration with biosynthetic databases [12]. In addition, BiG-SCAPE enables systematic exploration of BGC diversity in microbial communities and identification of rare and potentially novel clusters [3].

New opportunities for BGC validation and product characterization have emerged through robust heterologous expression systems. CRISPR-Cas9 genome editing has also been applied to directly activate silent BGCs in their native hosts, e.g., by promoter substitution, regulator overexpression, or terminator insertion [13,14]. The synthetic-bioinformatic natural product (syn-BNP) approach, which combines structure prediction with chemical synthesis, enabled the discovery of chisopeptin, a cationic cyclolipopeptide active against Gram-negative pathogens [15]. Cell-free protein synthesis (CFPS) enabled the production of embleporicin, the first class I lanthipeptide from actinobacteria, produced using this approach.

Metabolomics now enables the routine comprehensive profiling of microbial extracts. Liquid chromatography-tandem mass spectrometry combined with molecular networking tools such as GNPS (Global Natural Products Social Molecular Networking) enables visualization of chemical space and prioritization of novel metabolites [16]. Feature-based molecular networking integrates retention times, fragmentation patterns, and ion mobility data [17]. Stable isotope labeling approaches have directly linked metabolites to their BGCs; for example, $^{15}$N-nitrate feeding in *Nostoc* sp. enabled discovery of suomilide F and cyanopeptolin analogues [18]. The MassQL (mass spectrometry-based query language) workflow provided a programmable approach for targeted metallophore discovery from *Microbulbifer* spp. [19]. Combined-culture metabolomics with molecular networking revealed harundomycin A, a bifunctional conjugate produced only during co-culture of *Streptomyces hygroscopicus* and *Tsukamurella pulmonis* [20].

The application of artificial intelligence tools has become increasingly important in natural product discovery. PARAS (Prediction of Adenylation Domain Substrates) enables precise prediction of NRPS substrate specificities [11]. Phylogeny-guided natural product discovery,

which leverages evolutionary divergence within conserved biosynthetic enzymes, enabled the identification of mandimycin by constructing a phylogenetic tree of mycosamine-transferring glycosyltransferases from 316,123 bacterial genomes [21]. These tools continue to evolve, accelerating discovery workflows and guiding researchers toward the most promising BGCs.

## Peptides synthesized ribosomally and modified post-translationally (RiPPs)

Between 2023 and 2026, many novel compounds were identified in the lasso peptide, lanthipeptide, graspetide, sactipeptide, and other RiPP families. RiPPs originate from genetically encoded precursor peptides that are extensively modified in the post-translational stage to produce mature natural products, as shown in **Figure 1**.

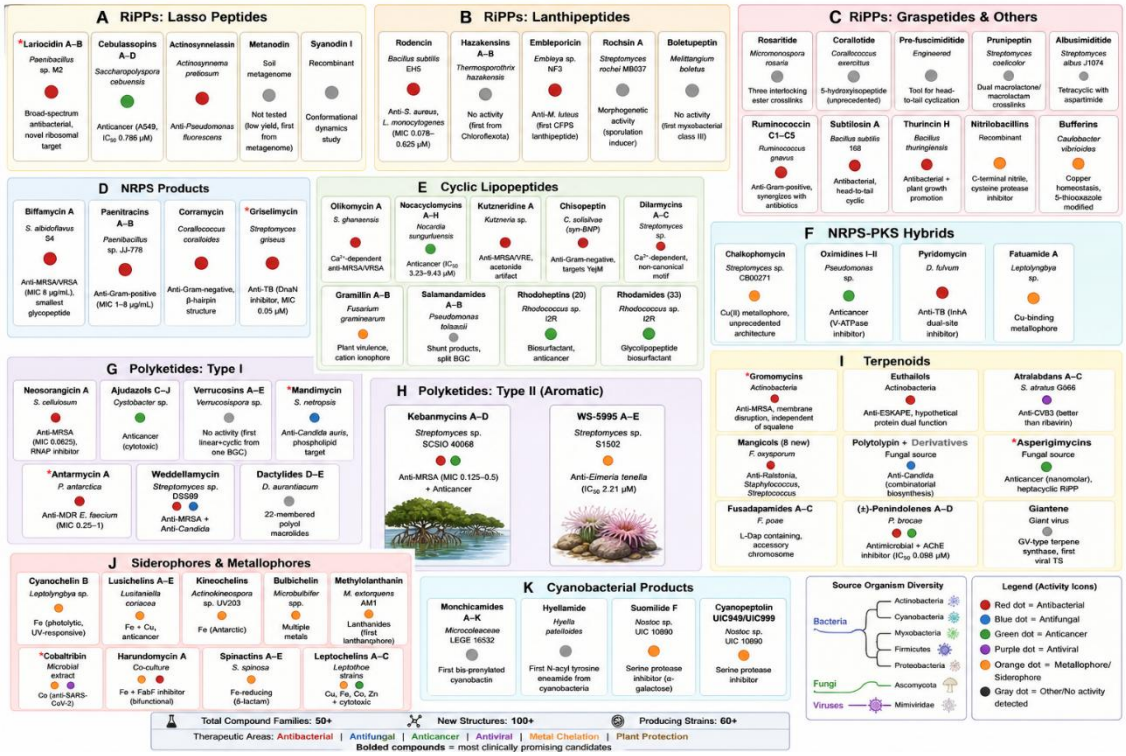


Figure 1. Microbial natural products discovered (2023–2026). Comprehensive summary of compounds organized by biosynthetic class across 11 categories. Compounds are color-coded by primary biological activity: red (antibacterial), blue (antifungal), green (anticancer), purple (antiviral), orange (metallophore/siderophore), and gray (no activity detected or other).

### Lasso peptide

Lasso peptides are characterized by a macrolactam ring formed by an isopeptide bond between the N-terminal amine and a side chain carboxylate. The C-terminal tail passes through this ring, forming a mechanically interlocked topology [22]. The lasso architecture gives these peptides excellent thermal and proteolytic stability [23], making them promising candidates for therapeutic development [22,24,25].

#### *Lariocidin*

Lariocidin is a lasso peptide antibiotic purified from *Paenibacillus* sp. One of the most important recent natural product discoveries is M2, a bacterium isolated from a soil sample from Hamilton, Ontario [26,27]. Lariocidin belongs to the class of ribosomally synthesized and post-translationally modified peptides with a knotted, slipknot-like fold [26]. Importantly, this is the first known lasso peptide that targets the bacterial ribosome [26,28]. The peptide is 18 amino acids long and contains an 8-residue macrolactam ring that threads and traps the remaining 10-residue C-terminal tail, creating the characteristic lasso topology. Another internally cyclized derivative, lariocidin B, was also discovered [26].

The mechanism of action of lariocidin is of particular interest. It binds to a completely new pocket in the small ribosomal subunit, unlike classical antibiotic binding sites such as tetracyclines or macrolides [26,28]. Structural, genetic, and biochemical data suggest that lariocidins sit between the 16S ribosomal RNA and the aminoacyl-tRNA, physically blocking the translocation step of protein synthesis and inducing miscoding [26]. This novel mode of action enables the molecule to escape common resistance mechanisms that compromise other ribosome-targeting drugs. A low propensity to generate spontaneous resistance under laboratory conditions, a promising marker for its clinical durability, supports this further [26].

Lariocidin demonstrated potent broad-spectrum antibacterial activity against a range of Gram-positive and Gram-negative pathogens, including multidrug-resistant strains. Crucially, it was not toxic to human cells, passing an important early stage of drug development. In a mouse model of infection with *Acinetobacter baumannii*, a top priority pathogen on the WHO list, Lariocidin showed strong protection in vivo, with animals treated with this peptide surviving and control animals dying [26].

Of course, the bacterium that makes the weapon has to be protected from the weapon itself. In a second study [29], the exact self-resistance mechanism was described. Adjacent to the lariocidin biosynthetic gene cluster is a gene encoding LrcE, an N-acetyltransferase of the GCN5-related N-acetyltransferase (GNAT) superfamily. LrcE catalyzes site-specific acetylation of a key lysine residue in the lariocidin tail. This single chemical modification destroys the antibiotic's activity, while the producer is rendered immune by disruption of ribosomal binding [29]. Fortunately, bioinformatic analysis of genomic databases indicated that LrcE homologues were present in environmental bacteria but largely absent from clinically important pathogens, alleviating concerns that resistance could readily be horizontally transferred to disease-causing organisms [29].

### *Cebulassopins*

Genome mining of the actinomycete *Saccharopolyspora cebuensis* SPE 10-1 identified cebulassopins A–D, the first lasso peptides produced from a split biosynthetic operon [46]. The precursor peptide genes (CbpA1–CbpA4) and maturation enzyme genes are encoded several megabase pairs apart, an architecture common in *Saccharopolyspora* but absent in related genera where intact BGCs are found [30].

Cultivation in R4-SW medium and chromatographic purification resulted in four lasso peptides. NMR analysis confirmed cebulassopin A to be a 15-residue lasso peptide with an 8-residue macrolactam ring (Gly-1-Asp-8 isopeptide bond), and cebulassopin B (2) to be a 16-residue lasso peptide with a 9-residue ring (Gly-1-Asp-9). All amino acids are of L configuration except D-arginine in 2. The threaded lasso topology was confirmed by the three-dimensional structure calculations using XPLOR-NIH [30]. Cebulassopins C and D were obtained but not fully characterized structurally [30]. ITC showed direct binding of the CbpA1 precursor and CbpB1 maturation enzyme even though they are separated in the genome. No disulfide bonds are present [30].

The most potent antiproliferative agent was Cebulassopin A, with an $IC_{50}$ value of 0.786 μM against A549 lung carcinoma cells, which was higher than that of etoposide ($IC_{50}$=2.571 μM). Cebulassopin B showed IC50 of 1.468 μM against A549 cells. Both compounds were not active against HCT116 colon, MDA-MB-231 breast, SNU-761 liver, and SNU-1105 glioblastoma cancer cells and WI-38 normal lung fibroblasts (IC50>100 μM), indicating selectivity for A549 cells [30]. No antimicrobial activity was found (MIC>200 μg/mL) [30].

Split-operon architecture indicates the possibility of independent regulation of precursor and maturation genes, thus reducing metabolic burden. This finding broadens the scope of RiPP genome mining, since precursor peptides may not be expected to be found next to their modification enzymes [30].

### *Actinosynnelassin*

Actinosynnelassin was identified from *Actinosynnema pretiosum* subsp. auranticum DSM 44131 via overexpression of an endogenous TetR/AcrR family regulator coupled with OSMAC-guided fermentation screening, which led to the activation of multiple silent secondary metabolite BGCs. The precursor gene *alnR/A* of the *aln* BGC encodes a 331 amino acid fusion protein comprising

an N-terminal AraC/XylS family transcriptional regulator (residues 1-290) fused to the lasso peptide leader and core sequences (residues 291-331), which is substantially larger than typical lasso peptide precursors [31].

The mature peptide was isolated directly from the native producer and structurally characterized by NMR (DQF-COSY, HSQC, HMBC, TOCSY, NOESY) [31]. Actinosynnelassin is a 17-amino acid lasso peptide that contains a 9-amino acid macrolactam ring (Gly-1–Asp-9 isopeptide bond), a 6-amino acid loop, and a 2-amino acid tail (Phe-17) [31]. The ring is sterically locked around the tail by three tryptophan residues (Trp-7, Trp-12, Trp-16). Mean global backbone RMSD: 0.20±0.10 Å [31]. The 3D structure was calculated using 509 distance restraints derived from NOEs. The core peptide sequence contains no cysteine residues, and no disulfide bond is formed [31]. Heat and protease stability experiments confirmed the characteristic lasso topology. The peptide retains its threaded conformation after heating at 95°C for 4 hours and degradation was observed only under combined heat and protease treatment [31]. Actinosynnelassin was active against a panel of Gram-positive bacteria and is the first lasso peptide described to inhibit *Pseudomonas fluorescens*. Six additional *aln*-like BGCs with the AraC–precursor fusion architecture were identified by comparative genomics in *A. pretiosum* ATCC 31280, *A. mirum* DSM 43827, *Streptomyces* sp. S465 and MG62, and *Thermomonospora echinospora* DSM 43163 [31].

### *Metanodin*

Metanodin is the first lasso peptide identified directly from a soil metagenome by a sequence-based method [32]. AntiSMASH mining of a metagenomic fosmid library from Schönbuch forest soil (Germany) showed 94 lasso peptide BGCs on contigs >5 kb, none of which matched any known MIBiG cluster [32]. Eight BGCs representing classical proteobacterial and nonproteobacterial ABC-type architectures were selected for heterologous expression in *Escherichia coli* [32].

Only BGC 89, refactored with a T7 promoter and optimized ribosome binding site, produced a detectable product [32]. Specifically, the precursor peptide gene was not detected by antiSMASH and required manual annotation [32]. The translated sequence contained a conserved threonine at the –2 position and an aspartate for the isopeptide bond formation. Still, an asparagine residue was present at the N-terminal ring-forming position, never observed before (glycine, cysteine, serine, or alanine are present in this position in known lasso peptides) [32].

Yields were too low for NMR or isolation [32], so high-resolution mass spectrometry was employed for structure confirmation. HCD fragmentation confirmed the C-terminal tail sequence (NIQGDHGLNI), and the random ring opening of the macrolactam resulted in nine linear peptides with 35 diagnostic b-ions that support the predicted ring sequence [32]. Interlocked fragment pairs confirmed the threaded lasso conformation [32]. The ring is a typical macrolactam with an isopeptide bond between Asn-1 and Asp-9 without heterocyclic modifications [32].

The native producer was identified taxonomically as an uncultivated bacterium belonging to the order Steroidobacterales (Gammaproteobacteria). Even the two similar BGCs had moderate similarity (B-gene: 53.50%; C-gene: 56.54%) and highly divergent core peptide sequences [32]. The production levels were not sufficient for bioactivity testing, demonstrating both the potential and current limitations of metagenomic lasso peptide discovery [32].

### *Syanodin I*

Syanodin I is a class II lasso peptide whose conformational landscape in solution and gas-phase was extensively characterized using an integrated structural biology workflow [33]. The peptide has been characterized by a combination of solution NMR spectroscopy, gas-phase hydrogen/deuterium back-exchange trapped ion mobility spectrometry–mass spectrometry (HDbX-TIMS-MS), electron capture dissociation (ECD), quantum mechanical calculations and molecular dynamics simulations [33].

Solution NMR analysis (600 MHz, $CD_3OH$, 283 K) showed syanodin I to be a 16-residue lasso peptide (Gly-1–Ala-16) containing a 9-residue macrolactam ring formed by an isopeptide bond between Gly-1 and Asp-9, a 4-residue loop (Ala-9–Gly-12) and a 4-residue C-terminal tail (Gln-13–Ala-16) [33]. Structure calculations were performed with X-PLOR using the CHARMM22 force field with a total of 101 NOE-derived distance restraints (35 intra-residue, 39

sequential, 27 medium-long range). The set of 15 lowest-energy structures had a backbone RMSD of 0.32±0.10 Å, and all residues were in most favored or additionally allowed regions of the Ramachandran plot [33]. Pro-10 is in a cis configuration [33].

The side chain of the plug residue Gln-13 forms a salt bridge to the C-terminal carboxylate, maintaining the lasso topology [33]. Fragmentation of the ECD displayed a maximum c•/c′ ratio at Ala-11 ($c_{11}$•) consistent with several long-range NOE correlations that identified Ala-11 as being in proximity to the macrolactam ring [33]. Syanodin I has no disulfide bonds and belongs to class II lasso peptides [33].

TIMS analysis resolved four distinct IMS bands for the [M + 2H]2+ ions of syanodin I and its branched-cyclic analog, within a similar collision cross-sectional window [33]. Solution-phase HDX-MS revealed mass shifts of around 17 deuteriums for the lasso form and around 20 deuteriums for the branched-cyclic form, consistent with the more folded character of the branched-cyclic C-terminal region [33]. HDbX-TIMS-MS experiments ($t_0 \approx 0.72$ ms to $t_9 \approx 865$ ms) resolved at least two different conformers in each IMS band, revealing intramolecular interactions not accessible to TIMS alone [53]. The QM calculations provided the HDX rate and number of accessible hydrogens for Pro-10 and Gln-13 and were used to assign the 2D-HDX-TIMS-MS data in an MD-based manner [33].

While this work does not provide any data on antimicrobial or biological activity [33], it provides a framework to examine biomolecular conformational dynamics using complementary solution- and gas-phase techniques.

## Lanthipeptides

Lanthipeptides are distinguished by thioether crosslinks (lanthionine and methyllanthionine) resulting from dehydration of serine or threonine residues and subsequent Michael-type addition of cysteine thiols. These crosslinks give lanthipeptides a rigid shape and protect them from enzymes, making them good scaffolds for drug development.

### *Rodencin*

Rodencin was isolated from *Bacillus subtilis* EH5, a balucin producer strain, by screening its class II lanthipeptide biosynthetic gene cluster [34]. The BGC encodes a two-component lanthipeptide system with α- and β-peptides, two dehydratases (RodM1 and RodM2), and a dehydrogenase (RodJA). RodJA is homologous to LanJ enzymes, which have previously been associated with the introduction of D-amino acids in lacticin 3147 [34].

The mature two-component peptide consisting of Rodα and Rodβ was produced by heterologous co-expression in a dedicated *Escherichia coli* system, and its modification was confirmed by MALDI-TOF mass spectrometry [34]. Tricine-SDS-PAGE analysis confirmed expression of the modified peptides and substrate specificity of the biosynthetic enzymes [34]. Rodencin has two different D-amino acids in the α-peptide (D-Ala) and the β-peptide (D-Ala and D-Abu) [34]. These are a rare modification in RiPPs, previously reported in lacticin 3147, but installed here by a distinct enzymatic system [34].

The dehydrogenase RodJA catalyzes the conversion of dehydroalanine to D-Ala and dehydrobutyrine to D-Abu. It works in conjunction with the dehydratases RodM1 and RodM2 that produce the dehydroamino acids from Ser and Thr residues, respectively [34]. The activity of these enzymes was reconstructed successfully in the *E. coli* heterologous expression system. To demonstrate the biosynthetic potential of this system, an analog of the D-amino acid-containing β-peptide of lacticin 3147 was produced using RodM2 and RodJA [34].

Rodencin has synergistic antimicrobial activity against food-borne pathogens. The combination of Rodα and Rodβ (1:1 ratio) showed MICs of 0.156 μM against *Staphylococcus aureus* LMG 8224 and *Listeria monocytogenes* LMG 10470, 0.078 μM against *Lactococcus lactis* NZ9000 and *Micrococcus flavus* NIZO B423, 0.625 μM against *Bacillus cereus* 14579 and *S. aureus* LMG 15975, and 5 μM against *Enterococcus faecium* LMG 16003 [34]. No activity was recorded against the Gram-negative bacteria *Escherichia coli* LMG 8223 and *Salmonella enterica* LMG 07233 (MIC >20 μM) [34]. No mechanistic studies, such as lipid II binding, fluorescence polarization, or human serum stability, were reported [34].

### *Hazakensins*

Hazakensins A and B were discovered through genome mining of the thermophilic bacterium *Thermosporothrix hazakensis*, which belongs to the class Ktedonobacteria in the phylum Chloroflexota [35]. Genome analysis identified a total of ten putative lanthipeptide biosynthetic gene clusters (five class I and five class II) [35].

Heterologous expression of a class I lanthipeptide BGC (BGC1) in *Escherichia coli* BL21(DE3) yielded two lanthipeptides, hazakensins A and B, which originate from two distinct precursor peptides (WP_170142646.1 and WP_170142645.1) encoded within the same cluster [35]. Co-expression with the cognate tRNA-Glu and glutamyl-tRNA synthetase genes from *T. hazakensis* increased the production yield of both peptides by approximately 4–6-fold [35]. The native strain *T. hazakensis* did not produce hazakensins A and B under the laboratory conditions tested, indicating that the BGC is cryptic in the wild-type organism [35].

The structures of hazakensins A and B, including the bridging pattern of lanthionine and methyllanthionine rings, were determined by extensive NMR analysis (DQF-COSY, TOCSY, NOESY, HSQC, HMBC) and mass spectrometry [35]. Hazakensin A is a 15-residue peptide (Ala-1 to Leu-15), and hazakensin B is a 13-residue peptide (Ala-1 to Leu-13), both containing the dehydrated amino acids 2,3-didehydrobutyrine and modified residues S-aminobutyric acid and S-alanine characteristic of lanthipeptides [35]. The two peptides have distinct amino acid sequences and are not simply variants differing by a single residue [35].

Antimicrobial activity testing revealed that both hazakensins A and B showed no inhibitory activity (MIC >64 μg/mL) against *Escherichia coli*, *Pseudomonas aeruginosa*, *Bacillus subtilis*, *Staphylococcus aureus*, and *Micrococcus luteus* [35]. No activity was reported against thermophilic bacteria. No thermal denaturation experiments, melting temperature determinations, or immunity protein studies were reported [35].

This work represents the first heterologous production of class I lanthipeptides originating from the phylum Chloroflexota and demonstrates that heterologous expression is an effective method to obtain lanthipeptides from cryptic BGCs of this under-explored bacterial lineage [35].

### *Embleporicin*

Embleporicin was discovered by genome mining of the endophytic actinobacterium *Embleya* sp. NF3 isolated from the medicinal plant *Amphipterygium adstringens* from Mexico [36]. AntiSMASH v. 7.1.0 analysis revealed three class I lanthipeptide BGCs in the genome. The chosen cluster (2.3) consists of 18 genes, spanning 24,462 nucleotides, including the precursor peptide gene *empA*, the dehydratase gene empB and the cyclase gene empC [36]. The EmpA precursor peptide comprises a 33-residue leader peptide with an LDLD motif, characteristic of class I lanthipeptides, and a predicted 26-residue core peptide with three serines, two threonines and four cysteines, potentially allowing for a four-ring cyclized peptide [36]. Embleporicin is not a member of the SCO0268 family of lanthipeptides and does not contain the PEAQxS motif but instead has a conserved GVQSxCxxCCx motif in the core peptide shared with other Embleya sequences [36].

The mature peptide was synthesized by cell-free protein synthesis (CFPS) using *E. coli* BL21(DE3) Star extract, the first class I lanthipeptide from actinobacteria produced using this approach [36]. The modified precursor peptide (mEmpA) was obtained by co-expression of the *empA*, *empB*, and *empC* genes in the presence of total RNA from Embleya sp. NF3 and $ZnCl_2$ as a cofactor for the cyclase EmpC. The leader peptide was cleaved by the Furin protease in vitro to release mature embleporicin [36]. Western blot analysis showed expression of EmpB (~118 kDa) and EmpC (~48.9 kDa); however, EmpB expression was significantly weaker than EmpC and may be a limiting factor in production [36].

No NMR and X-ray crystallography were carried out; structural characterization was restricted to bioinformatic prediction [36]. The lanthionine bridging pattern was not determined experimentally, and no labionin crosslinks were identified or proposed [36]. The EmpB enzyme exhibited the highest identity with actinobacterial lanthibiotic dehydratases PspB (32.1%), MibB (30.2%), and CebB (26.2%), whereas EmpC exhibited the highest identity with MibC (34.4%) and PspC (32.2%) [36].

Embleporicin showed antimicrobial activity against *Micrococcus luteus* ATCC 9341 with an inhibition halo equivalent to 90 IU of commercial nisin. Still, activity was only observed at high CFPS concentrations (concentrated from 600 µL of reaction) [36]. Antimicrobial activity was seen in samples boiled at 85 °C for 5 minutes, indicating heat stability [36]. No minimum inhibitory concentration values were determined, and no activity was reported against vancomycin-resistant enterococci, methicillin-resistant *Staphylococcus aureus*, or any other clinically relevant pathogens [36]. No vancomycin synergism studies, lipid II binding assays, or transglycosylation/transpeptidation inhibition experiments were done. [36]. As the authors mentioned, future work will be directed towards enhancing production efficacy and activity against multidrug-resistant Gram-positive and Gram-negative pathogenic strains [36].

### *Rochsin*

Rochsin A was discovered through genome mining of *Streptomyces rochei* MB037, an actinobacterium isolated from marine sponges [37]. The cryptic class III lanthipeptide biosynthetic gene cluster (*rcs*) was identified and heterologously expressed in Escherichia coli BL21(DE3) by co-expression of the precursor peptide RcsA (fused to an N-terminal SUMO-tag to prevent proteolysis) with the class III lanthipeptide synthetase RcsKC [37]. The native strain failed to produce rochsin A under the laboratory conditions tested [37].

The presence of the coupled labionin cross-links, a bicyclic structure containing C–C and C–S bonds, was confirmed by NMR analysis (700 MHz, DMSO-$d_6$) of the truncated rochsin A, which is characteristic of class III lanthipeptides [37]. Labionin was confirmed further by acid hydrolysis followed by derivatization and MS/MS analysis [37]. The highly rigid conformation is crowded with bulky aromatic amino acids [37]. Biosynthesis requires only one class III synthetase (RcsKC) that catalyses both dehydration and cyclization reactions [37]. Ala mutation experiments were conducted on Ser5, Ser8, Cys11, Ser12, Ser15 and Cys19 to define the direction of cyclization, which was found to be C-to-N, consistent with most class III lanthipeptides [37]. RcsKC also shows high substrate promiscuity, thus allowing diverse ring topologies rarely observed in other class III lanthipeptides [37]. Leader peptide removal was carried out by three AplP-like proteases (StrR037P5, P6 and P7) encoded outside of the *rcs* BGC, which display dual endo- and aminopeptidase activities and generated the mature core peptide in vitro [37].

Rochsin A was inactive against 24 marine-derived bacterial isolates and noncytotoxic against 15 human cancer cell lines at 20 µM [37]. However, the core peptide of rochsin A showed morphogenetic activity and induced morphological differentiation and sporulation of *S. rochei* MB037 at 20 µg [37]. No activity was reported against MRSA, *Streptococcus pneumoniae,* or *Staphylococcus aureus* biofilms, and no mechanism-of-action studies were performed using cell division or fluorescence microscopy [37].

### *Boletupeptin*

Boletupeptin was isolated by genome mining of the myxobacterium *Melittangium boletus* DSM 14713 [38]. A Blastp search with a class III lanthipeptide synthetase as query identified the gene *bolKC* for the modification enzyme, and a gene *bolA* for a precursor peptide was manually annotated in the upstream region, because it was not present in the original database annotation [38]. The *bolA* gene encodes a 45 amino acid precursor peptide containing the conserved Lab-forming motif SxxSxxxC and a long C-terminal tail sequence (ADGGTTPPASK) [38].

A new class III lanthipeptide, boletupeptin, was produced by heterologous co-expression of codon-optimized *bolA* and *bolKC* in *Escherichia coli* BL21 (DE3) with the pET-29b (+) vector at a yield of 0.5 mg per 1 L culture [38]. The native strain did not produce detectable amounts of boletupeptin under the conditions tested [38]. Accurate mass spectrometry [38] gave the molecular formula $C_{45}H_{73}N_{11}O_{16}S$. The structure elucidation was based on CID-MS experiments following $NaBH_4$ reductive cleavage, which demonstrated the presence of one unit of labionin and identified the C-terminal sequence as Ala-Asp [38]. The 1H NMR spectrum was too broad for detailed analysis [38]. Site-directed mutagenesis experiments showed that at least three amino acids (ADG) in the C-terminal tail are required for successful lanthipeptide production [38].

Boletupeptin showed no antibacterial activity against *E. coli*, *P. aeruginosa*, *B. subtilis*, *M. luteus*, and *S. aureus* at 64 µg/mL or against the myxobacterial strains *Melittangium lichenicola*,

*Corallococcus coralloides,* or *Myxococcus fulvus* at 2 μg [38]. This is the first class III lanthipeptide from a myxobacterial source [38].

## Graspetides

Graspetides are distinguished by ATP-grasp enzyme-facilitated ω-ester or ω-amide side chain–side chain crosslinks, yielding macrocyclic peptides [39]. From 2023 to 2024, studies expanded our understanding of graspetide biosynthesis and engineering, including the discovery that the ATP-grasp enzyme ThfB can catalyze thioester cross-link formation, enabling a recombinant route to head-to-tail cyclic peptides via native chemical ligation [39,40].

### *Rosaritide and corallotide*

Rosaritide and corallotide were discovered by a large-scale bioinformatic analysis of graspetide biosynthetic gene clusters using an updated version of the genome-mining tool RODEO [41]. The analysis surveyed available genomic data and identified >20,000 predicted graspetides across 19 new groups [41]. This analysis prioritized two groups of graspetides for characterization with strictly conserved co-occurring proteins of previously unknown function. The BGC for rosaritide is derived from *Micromonospora rosaria* NRRL 3718, a soil actinobacterium, and encodes the graspetide synthetase MirB and a putative PpiC-type peptidylprolyl isomerase, MirC, as the partner protein [41]. The corallotide BGC is from *Corallococcus exercitus* and encodes the graspetide synthetase CorB, the divergent 2OG-Fe (II)-dependent oxygenase CorC, and a β-lactamase CorD [41].

Heterologous expression in *Escherichia coli* showed that the graspetide synthetases need their respective partner proteins to be active [41]. When the precursor peptide MirA was co-expressed with only the synthetase MirB, no modifications were observed. In contrast, three dehydrations (corresponding to three graspetide linkages) were only observed upon co-expression with MirB and MirC [41]. CorB was again needed for full activity, but CorC alone was active and stable [41]. Although the MirB and MirC proteins were individually unstable, they formed a catalytically active complex upon coexpression and copurification [41]. This partner-dependent biosynthesis is a novel regulatory mechanism in the assembly of the graspetide [41].

Structural characterization using 2D NMR (COSY, TOCSY, NOESY, HSQC) determined that rosaritide contains three interlocking macrolactone (ester) linkages, instead of amide linkages, formed between Ser/Thr donor residues and Asp acceptor residues, and that Pro-16 and Pro-21 are present in the trans conformation [41]. The ring connectivity is a new interlocking pattern of the graspetides [41]. Corallotide contains five repeated motifs in which a Lys is first macrocyclized into an isopeptide bond with an Asp and then hydroxylated at the δ-carbon by CorC to form a 5-hydroxyisopeptide moiety, which is unprecedented in natural products [41]. It is not a single macrocycle of 14 residues but five different cyclized motifs within a large precursor peptide [41]. For either compound, no antioxidant activity, DPPH radical scavenging, or hydrogen peroxide protection assays were reported. No substantial growth inhibition was observed in disk diffusion assays against *Escherichia coli*, *Bacillus subtilis*, *Sorangium cellulosum* and *Micrococcus luteus* [41].

### *Pre-Fuscimiditide*

Pre-fuscimiditide is a 22-amino acid graspetide with two ester cross-links resulting in a stem–loop structure, installed by a single ATP-grasp enzyme, ThfB [42]. In addition to the native ester cross-links, ThfB was shown to catalyze amide or thioester cross-link formation in pre-fuscimiditide variants, with thioester formation being particularly efficient [42]. The thioester-linked peptide is rapidly and quantitatively rearranged by native chemical ligation to an isopeptide-bonded head-to-tail cyclic peptide once the N-terminal cysteine residue is exposed by proteolytic cleavage, and the solution structure of this cyclic peptide was determined by 2D NMR spectroscopy [42]. This provides an easy recombinant route to head-to-tail cyclic peptides [42].

Subsequent studies showed that ThfB has a broad substrate promiscuity, allowing insertions of up to 72 amino acids in the loop and even whole proteins like mRuby2, sfGFP and mTurquoise2 [42]. Cyclized constructs maintained the trypsin resistance observed for the wild-type pre-fuscimiditide, and cyclization of mRuby2 did not affect its fluorescence or thermostability [42].

ThfB was also shown to covalently crosslink a non-covalently associated coiled-coil protein pair, further demonstrating its versatility as a protein cyclization biocatalyst [42].

### *Prunipeptin*

Prunipeptin is a group 11 graspetide from *Streptomyces coelicolor* containing both the macrolactone and macrolactam cross-links, installed by a single ATP-grasp cyclase, PruB [43]. Recombinant PruA and PruB were used to reconstitute prunipeptin biosynthesis in vitro, and tandem MS analysis identified a bicyclic core peptide [43]. PruB had a Km of 24.3±9.1 μM and a kcat of 39.3±0.9 $min^{-1}$ (higher kcat due to use of an ATP-regeneration system) and bound PruA with a Kd of 2.4–4.0 μM, determined by microscale thermophoresis [43]. The crystal structure of PruB was solved by X-ray crystallography at a resolution of 2.91 Å and displayed different electrostatic surface features from those of group 1 and 2 graspetide [43]. Site-directed mutagenesis showed that the conserved DxR motif (Asp-231), ATP/Mg2+-binding residues, and residues involved in leader and core peptide binding are essential [43]. Computational modeling and molecular dynamics simulations of the PruA/PruB co-complex suggested that PruB first catalyzed the macrolactone bond formation on PruA, providing mechanistic insights into the dual macrocyclization activity of graspetide synthetases [43].

### *Graspimiditides and albusimiditide*

Graspimiditides are a subgroup of graspetides, containing an additional aspartimidylation post-translational modification catalyzed by an O-methyltransferase, and are mostly found in actinobacterial genomes [44]. A comprehensive bioinformatic analysis of 5,000 methyltransferase homologs identified 962 unique putative graspimiditides grouped into eight major clusters, with cluster 1 being the largest (641 members) and encoded almost exclusively in Streptomyces [44]. Fuscimiditide was a singleton, and amycolimiditide clustered in cluster 5 [44]. Albusimiditide from *Streptomyces albus* J1074 was characterized as a representative of cluster 1 and was found to be a 46-residue tetracyclic peptide with four ω-ester linkages forming a stem–loop structure containing one aspartimide [44]. The ester cross-links are 22-, 46-, 22- and 44-atom macrocycles, with the largest macrocycle containing the aspartimide, which hydrolyzes in a 3:1 ratio of isoaspartate to aspartate residues [44].

## Sactipeptides and thioether-containing RiPPs

Sactipeptides are defined by sulfur-to-α-carbon (sactionine) thioether crosslinks formed by radical SAM (rSAM) enzymes [45,46]. During the years 2023 to 2026, genome mining efforts expanded the known diversity of this class.

### *Ruminococcin C*

The Ruminococcin C (RumC) sactipeptides are a family of five isoforms (RumC1–C5) produced by the Gram-positive human gut symbiont *Ruminococcus gnavus* E1, co-expressed with two radical SAM maturases [47]. RumC1 was previously demonstrated to be active against a panel of multidrug-resistant Gram-positive clinical isolates [47]. After adapting the biosynthesis protocol to obtain the four additional mature isoforms (RumC2–5) [47], both maturases were shown to tolerate the different precursor peptides. All five isoforms were safe for human cells and had different antibacterial effects [47]. We did not observe any synergy among the five RumCs; however, synergistic action was demonstrated with conventional antibiotics targeting the cell wall, and important residues for antibacterial activity were identified [47].

### *Subtilosin A*

Subtilosin A is a 35-residue head-to-tail cyclic sactipeptide first isolated from *Bacillus subtilis* 168 with three sactionine thioether crosslinks catalyzed by the radical SAM enzyme AlbA [48]. This biosynthesis is regulated by the *sbo-albABCDEFG* gene cluster, where AlbE and AlbF are involved in the leader peptide cleavage and macrocyclization, and AlbC is responsible for export [48]. A group of researchers was able to reconstitute subtilosin A biosynthesis in *Escherichia coli* by co-expressing SboA with AlbA, AlbE, and AlbF and showed that both AlbE and AlbF are required for head-to-tail macrocyclization. An open-chain analog lacking macrocyclic structure but retaining the thioether crosslinks was detected and designated subtilosin AOC, a probable biosynthetic

precursor, and showed a marked reduction in antibacterial activity relative to the mature subtilosin A [49]. Recent comparative genomics of 6815 *Staphylococcus pseudintermedius* isolates further demonstrated that the subtilosin A BGC is part of the accessory genome, conserved in subsets of clinical and environmental isolates [48].

### *Thurincin H*

Thurincin H is an anionic sactipeptide with 31 amino acids produced by *Bacillus thuringiensis* with a molecular weight of 3139.51 Da and four sactionine thioether crosslinks [50,51]. It exhibits antimicrobial activity mainly against Gram-positive bacteria, which includes foodborne pathogens and phytopathogens [50]. Thurincin H has been reported to act as a signaling molecule that induces plant growth, particularly under stress conditions, in addition to its antimicrobial activity, and shows biotechnological potential [50]. Its biotechnological application is greatly limited by low production yield, mainly attributed to the complexity of its biosynthesis, which also makes attempts for heterologous expression difficult [50].

## Nonribosomal peptide synthetase (NRPS) products and hybrids

NRPSs are large enzymes that assemble complex peptides by a thiotemplate mechanism.

### NRPS-derived antibiotics

### *Paenitracins*

Paenitracins A and B constitute a novel family of bacitracin-type nonribosomal peptide antibiotics discovered using a targeted mass spectrometry (MassQL)-based metabolomics approach from 227 plant-associated *Paenibacillus* isolates [52]. The compounds were isolated from *Paenibacillus* sp. JJ-778 and represent the first reported bacitracin-type peptides from the genus *Paenibacillus* [52]. Genome sequencing and antiSMASH analysis revealed a 12-module NRPS gene cluster with 77% similarity to the bacitracin BGC of *Bacillus licheniformis* [52].

Structural elucidation by NMR and Marfey's analysis showed paenitracins to be macrocyclic dodecapeptides with an N-terminal thiazoline moiety, differing from canonical bacitracins by three amino acid substitutions: Leu instead of Orn at position 7, Trp instead of Phe at position 9, and Thr instead of His at position 10 [52]. Paenitracins A and B are diastereomers, most likely differing in the stereochemistry of the N-terminal Ile residue [52].

Paenitracin B showed antibacterial activity against Gram-positive pathogens, with MIC values of 1–8 μg/mL (0.7–5.6 μM) against *Staphylococcus aureus* ATCC 29213, *S. aureus* USA300, *Enterococcus faecium* E155, and *E. faecium* E980, comparable to commercial bacitracin. In contrast, no activity was observed against *Escherichia coli* ATCC 25922 [52]. Antagonization assays confirmed that the interaction of paenitracin A with undecaprenyl pyrophosphate (C55PP) is zinc-dependent, consistent with the established mode of action of bacitracins [52].

### *Corramycin*

Corramycin is a novel zwitterionic modified peptidic antibiotic isolated from the myxobacterium *Corallococcus coralloides* and active against several Gram-negative pathogens [53,54]. The peptide contains several modified amino acids, an N-terminal butyric acid, and a γ-N-methyl-β-OH-histidine, and the biosynthetic gene cluster is a 12-modular hybrid NRPS–PKS megasynthetase. The crystal structure of corramycin in complex with the self-resistance kinase ComG shows that the antibiotic adopts a β-hairpin-like conformation stabilized by six intramolecular hydrogen bonds and no disulfide bridge [54]. ComG, encoded within the corramycin BGC, phosphorylated and inactivated corramycin at the β-alanine moiety in an ATP-dependent manner, providing self-resistance; ComG is structurally similar to aminoglycoside phosphotransferases but does not display activity against aminoglycosides, and bioinformatic analyses revealed a limited occurrence of ComG-like proteins with no evidence of pre-existing resistance in pathogenic bacteria [54].

The first natural product showed a limited antibacterial spectrum and moderate MICs, but an optimization program based on Ala-scanning of the peptidic part, stabilization and incorporation of primary amine or siderophore groups gave corramycin 28 with a better mouse IV pharmacokinetic profile, a broader Gram-negative spectrum and outstanding efficacy in several in vivo mouse infection models [53]. A modular total synthesis was realized by two consecutive chemical ligations using Ser/Thr ligation in combination with classical fragment coupling [55]. To date, the exact mechanism of action of corramycin has not been elucidated [54].

### *Griselimycin*

Griselimycin is a cyclic depsipeptide first isolated from *Streptomyces griseus* in the 1960s [56,57]. It is composed of ten residues, an eight-residue macrocycle cyclized by an ester bond between the side chain of Thr3 and the C-terminus of Gly10, and a two-residue tail with an acetylated N-terminus. Although its development was initially stopped due to poor pharmacokinetic properties, the compound has regained interest as a promising anti-tubercular lead [56–58].

Mechanistic studies identified the DNA sliding clamp (DnaN, the β subunit of DNA polymerase III) as the target of griselimycin, an essential component of the bacterial DNA replication machinery [56,57]. A large-scale structural genomics effort solved fifteen crystal structures of β-clamp orthologs, including eight cocrystal structures with griselimycin, which revealed that the peptide binds at a conserved hydrophobic patch between domains II and III, with its macrocyclic ring occupying subsite 1 and its linear segment at subsite 2 of the polymerase binding site [56]. Binding affinity measurements showed KD values between 7 and 496 nM for a range of Gram-negative β-clamp orthologs, while *Mycobacterium tuberculosis* DnaN bound too tightly for accurate measurement [56].

Griselimycin has potent activity against *M. tuberculosis,* with the natural product having a MIC of 0.9 μM and the cyclohexyl derivative (CGM) improving to 0.05 μM [57]. As expected, Leu4 was least tolerant to substitution because of the deep burial of its side chain in a hydrophobic pocket in DnaN. In contrast, exocyclic residues Me-Val1 and Pro2 were most tolerant to modification based on an extensive alanine scan and structure–activity relationship analysis [58]. The N-terminus was a promising target for derivatization, with a fluorophore-labeled analogue retaining activity and allowing visualization of griselimycin accumulation inside mycobacteria within macrophage phagosomes [58]. The activity of griselimycin against Gram-negative bacteria is limited by poor DnaN binding affinity, evidenced by the fact that *E. coli* DnaN is bound 8,000-fold weaker than *M. smegmatis* DnaN [56,58].

### *Biffamycin A*

Biffamycin was discovered from genome mining of an environmental isolate of *Streptomyces albidoflavus*. The BGC from *Streptomyces albidoflavus* S4 harbors a unique two-module NRPS with a C-terminal SurE domain suggested to promote peptide release via macrocyclization through amide bond formation. The mature peptide was produced by de-regulation of the native promoter in *S. albidoflavus* S4 and was studied by NMR and MS. Biffamycin A is a glycotetrapeptide, a rare class of natural product that is a cyclic tetrapeptide containing a 3-hydroxy(α-D-mannosyl)-D-lysine moiety and a 5-chloro-4-methoxy tryptophan moiety. Biffamycin A is active against drug-resistant *Staphylococcus aureus*, including MRSA and VRSA (MIC 8 μg/mL), and *Mycobacterium smegmatis* (MIC 16 μg/mL), with minimal activity against Gram-negative bacterial strains [57]. It was not effective against *M. avium* complex and *M. tuberculosis* in the present study [57]. The precise mechanism of action remains unknown, although activity against VRSA indicates that it has either a different mode of action than vancomycin or circumvents VanA-mediated resistance.

## Cyclic lipopeptides

Cyclic lipopeptides are composed of a cyclic peptide moiety and a fatty acid chain. This confers amphiphilic properties, allowing them to interact with membranes.

### *Olikomycin A*

Olikomycin A was identified by knocking out the global regulator wblA in *S. ghanaensis* ATCC 14672, resulting in the activation of a silent 92 kb BGC containing four NRPS genes [61]. It is a

cyclic lipodepsipeptide, consisting of a (2Z,4E)-8-methylnona-2,4-dienoic acid chain and 14 amino acids linked by an ester bond. The compound does not contain the canonical Asp-X-Asp-Gly calcium-binding motif but has an Asp10-Gly11-(D-allo-Thr)12-Ala13 sequence. It is active against MRSA and VRSA (MIC 1–2 μg/mL with $Ca^{2+}$), but much less active in the absence of calcium (MIC 32 μg/mL). Olikomycin A similarly disrupts membrane integrity to daptomycin and is non-cytotoxic to CHO-K1 and HepG2 cells up to 37 μg/mL [6,59,60].

### *Nocayclomycins*

The OSMAC approach in combination with genome analysis led to the identification of nocacyclomycins A–H from *Nocardia sungurluensis* YINM00009 [61]. The compounds were isolated directly from the producing strain and not by promoter engineering. Their structures, including absolute configurations, were elucidated by NMR, HRESIMS/MS, X-ray crystallography and Marfey's method, and they were found to be cyclic lipodepsipeptides. Bioinformatic analysis allowed us to propose a biosynthetic pathway. Biological evaluation of compounds 5 and 7 showed significant cytotoxic activities against four human cancer cell lines (A549, HepG2, MDA-MB-231, and SW480) with $IC_{50}$ values of 3.23–9.43 μM and negligible cytotoxicity in normal cells [61].

### *Kutzneridine A*

Genome mining of *Kutzneria* sp. resulted in the identification of Kutzneridine A. CA-103260, genus not yet identified for lipopeptide production [62]. The BGC was cloned into a BAC and heterologously expressed in *Streptomyces coelicolor* M1152. The compound is a cyclic lipo-tetrapeptide containing two diaminopropionic acid residues and an N,N-acetonide ring, which was found to be an artifact from the acetone used in isolation. Kutzneridine A exhibited strong antibacterial activity against methicillin-resistant *Staphylococcus aureus* and vancomycin-resistant *Enterococci* [62]. It does not contain 4-hydroxyproline, 3-hydroxyaspartic acid, or chlorinated tryptophan as it was first reported [60].

### *Chysopeptins*

Chisopeptin was discovered by two-round motif-driven genome mining of 8,982 genomes from 42 under-investigated Gram-negative bacterial genera for BGCs encoding cationic cyclolipopeptides with multiple D-amino acids [15]. *Chitinophaga solisilvae* BGC was not heterologously expressed; rather, a synthetic-bioinformatic approach using SPPS was used. Chisopeptin is a 12-residue cyclic lipopeptide containing a tetradecanoic acid chain and six positively charged amino acids. It is active against Gram-negative pathogens, including *K. pneumoniae* and *E. coli* (MIC 2–8 μg/mL), but it is inactive against Gram-positive bacteria. Mechanistic studies indicate that it targets YejM, an inner membrane protein that regulates LPS biogenesis [15].

### *Dilarmycines*

Genome mining of *Streptomyces* sp. CA-278952 resulted in the identification of dilarmycins A–C, a lipopeptide with an Asp-Gly-Glu-Ala motif [63]. This motif was designed to mimic the canonical Asp-X-Asp-Gly motif of calcium-dependent lipopeptide antibiotics. Chemical analysis of the producing strain resulted in the identification of three new lipodepsipeptides, dilarmycins, which exhibited calcium-dependent antibacterial activity against Gram-positive pathogens, including methicillin-resistant *Staphylococcus aureus* and vancomycin-resistant *Enterococcus* [63]. The compounds constitute a new structural class of calcium-dependent antibiotics, with a non-canonical calcium-binding motif, distinct from the conserved Asp-X-Asp-Gly pattern [60].

## NRPS-PKS hybrids

NRPS–PKS hybrid molecules combine modules from both assembly line systems to generate molecules with peptide–polyketide backbones.

### *Chalkophomycine*

Chalkophomycin, a natural product with an unprecedented molecular architecture with an asymmetric square-coordination system, was obtained from *Streptomyces* sp. CB00271, a Cu (II)

binder [64]. Genome mining for homologues of the N-nitrosating enzyme SznF in *Streptomyces anulatus* ATCC 11523 resulted in the identification of the BGC (chm) among more than 400 cryptic BGCs [65]. Chalkophomycin has a C-type diazeniumdiolate and an N-hydroxypyrrole moiety. The N-hydroxypyrrole is biosynthesized from L-proline via two flavin-dependent enzymes, ChmG and ChmH, the first characterized prolyl-N-hydroxylase [65]. Chalkophomycin is a metallophore for copper (II), and its unusual coordination chemistry may inspire the development of therapeutic chelators for neurodegenerative diseases or antitumor agents [64]. The supplied publications did not report any antibacterial or antimycobacterial activity.

### *Oximidinas*

Oximidines I and II were isolated from Pseudomonas sp. Q52002 as 12-membered macrolides with an unusual O-methyloxime moiety [66]. They selectively inhibited the growth of rat 3Y1 cells transformed with E1A, ras, or src oncogenes. Later, the biosynthetic gene cluster was identified in *Pseudomonas baetica,* revealing a trans-AT polyketide synthase pathway [67]. O-methyloxime formation proceeds via a novel mechanism catalyzed by a specific monooxygenase and methyltransferase domain in the PKS assembly line. Four more oximidine derivatives were characterized, including a structurally simpler intermediate that has potent anticancer activity [67]. Compounds inhibit the vacuolar H+-ATPase. No antibacterial activity against Gram-positive or Gram-negative bacteria was reported in the provided publications. Oximidines are described as anticancer agents.

### *Pyridomycine*

Pyridomycin was originally discovered from *Dactylosporangium fulvum* with cidal activity against mycobacteria [68]. Later, it was found in *Streptomyces* sp. W3009 [69]. This cyclodepsipeptide is rich in 3-(3-pyridyl)-L-alanine (3-Pal), which is biosynthesized by a concerted NRPS-PKS hybrid system where nicotinic acid and 1,3-bisphosphoglycerate are condensed by the type I PKS enzyme Pyr9 [70]. Pyridomycin inhibits the enoyl reductase InhA through a novel dual-site inhibition mechanism that uniquely bridges both the NADH- and substrate-binding pockets [68]. Susceptible to isoniazid-resistant clinical isolates. Pyridomycin is a potent anti-mycobacterial agent but suffers from poor metabolic stability. Improved-stability semisynthetic derivatives were obtained, but pyridomycin and its analogs did not show efficacy in a murine tuberculosis model [71]. Linear derivatives with the 3HP–T–3PA scaffold were inactive [69].

## NRPS of split BGCs: Salamandamides

Salamandamides A and B, a new class of linear lipodipeptides, were recently isolated from *Pseudomonas tolaasii* RSB 5.11 [72]. Salamandamide A is a lipid moiety N-terminally linked to two amino acids, L-leucine and L-glutamine, and is a 3-hydroxydecanoic acid (3-HDA). Interestingly, these compounds were inactive in the antimicrobial, antifungal, and cytotoxicity assays. Genome mining and knockout experiments showed that salamandamides do not possess a specific biosynthetic gene cluster, despite their structural heterogeneity. They are rather biosynthetic intermediate shunt products of the nonamodular NRPS assembly line of the viscosin family, i.e., the pseudodesmin cluster. These assembly lines typically give rise to cyclic lipononapeptides but also can release smaller linear dipeptide fragments in the early biosynthetic stages. This biosynthesis is characterized by a split-NRPS or bipartite BGC structure with structural genes located at separate genomic loci. The pseudodesmin cluster in *P. tolaasii* RSB 5.11 comprises a single stand-alone bimodular NRPS (PdmA) and a single stand-alone heptamodular NRPS (PdmB/C). This split architecture creates a biosynthetic breaking point, enabling PdmA to operate independently in producing and releasing linear salamandamide lipopeptides [72].

## Polyketides

Polyketides are a large family of structurally diverse natural products that are biosynthesized by polyketide synthases (PKSs) via sequential decarboxylative condensations of acyl-CoA building blocks, usually malonyl-CoA and methylmalonyl-CoA. These enzyme complexes are like fatty acid synthases, but they expand structural diversity by changing the selection of starter units, chain

elongation, and post-assembly modifications. There are three main types of PKSs: type I (large, modular megasynthases), type II (dissociated, iterative enzyme complexes), and type III (homodimeric, iterative enzymes). Polyketides include many clinically important antibiotics (erythromycin, tetracyclines), anticancer agents (doxorubicin) and immunosuppressants (rapamycin).

### *Neosorangicin A*

Neosorangicin A was discovered through activity-guided fractionation of the myxobacterium *Sorangium cellulosum* strain Soce439, not through genome mining [73]. It is a macrolide-polyether antibiotic belonging to the sorangicin family. The compound was isolated directly from the native producer; no heterologous expression in *Myxococcus xanthus* was reported. Neosorangicin A shares the same macrolactone core as sorangicin A but features a shortened side chain with a secondary alcohol at C-5 and lacks the terminal carboxylic acid. Its biosynthetic gene cluster (*nsr*) spans 124.3 kb and closely resembles the sorangicin BGC. Neosorangicin A exhibited strong activity against Gram-positive bacteria, including MRSA (MIC 0.0625 μg/mL), and potent activity against *Mycobacterium tuberculosis* (MIC 1.6 μg/mL). It targets bacterial RNA polymerase (RNAP), as confirmed by in vitro $IC_{50}$ measurements (0.31 μg/mL against *S. aureus* RNAP), and shares overlapping binding sites with rifampicin. Despite enhanced in vitro potency, neosorangicin A failed to show in vivo efficacy in a murine wound infection model due to rapid degradation in mouse plasma (half-life <0.5 min) [73].

### *Ajudazols C–J*

Ajudazols C–J were discovered from *Cystobacter* sp. SBCb004 through mutagenesis and metabolomics analyses of a truncated ajudazol biosynthetic gene cluster, not from *Sorangium cellulosum* [74]. Unlike ajudazols A and B, which utilize acetyl-CoA as the starter unit, these novel derivatives incorporate 3,3-dimethylacrylyl-CoA. The new ajudazols are characterized by varying degrees of hydroxylation, desaturation, and different glycosylation patterns. Mutagenesis studies revealed that two P450-dependent enzymes catalyze hydroxylation at C-8 and desaturation at C-15 and C-33, while a glycosyltransferase transfers a D-β-glucopyranose moiety. Notably, one P450 enzyme and the glycosyltransferase are encoded outside the BGC. The structures were elucidated using comprehensive HR-MS and NMR spectroscopy. Ajudazols C–H exhibited cytotoxicity against various cancer cell lines. No mitochondrial complex I inhibition or specific $IC_{50}$ values of 2–20 nM against pancreatic cancer cell lines were reported in the provided publication [74].

### *Mangicol sesterterpenoids*

Mangicol sesterterpenoids were originally isolated from the marine fungus *Fusarium heterosporum*, with eight new derivatives recently discovered from *Fusarium oxysporum* 14005 through genome mining, heterologous pathway reconstitution in *Aspergillus oryzae*, and feature-based molecular networking [75]. A newly identified bifunctional terpene synthase is responsible for mangicol biosynthesis. The new mangicols feature epoxy and tetrahydrofuran moieties on their side chains. Antimicrobial assays revealed potent activity against *Ralstonia solanacearum*, *Staphylococcus aureus*, and *Streptococcus mutans*, with MICs ranging from 6.25 to 25 μM. No activity against *Candida albicans* was reported. Three compounds demonstrated significant antineuroinflammatory effects in murine BV2 microglial cells, reducing inflammation by 48–53%. NF-κB signaling inhibition was not reported as the mechanism of action in the provided publication [75].

### *Verrucosins*

Verrucosins A–E were isolated from the marine actinobacterium *Verrucosispora* sp. strain TAA-831, collected in the Northern Marianas Islands, not through genome mining [76]. The compounds were obtained through large-scale fermentation and targeted isolation, not heterologous expression. Verrucosins A and B are linear 3,5-dihydroxybenzenic polyketides, while verrucosins C–E are carbocyclic macrocycles of the ansamycin type. Targeted genome mining revealed a single type I/type III hybrid PKS BGC (*vrs*) responsible for producing both linear and cyclic congeners, representing the first demonstration that a single BGC can naturally produce both structural classes. The verrucosins lack significant antibiotic activity; they were

inactive against methicillin-resistant *Staphylococcus aureus* and *Escherichia coli* in agar disk diffusion assays. No antimycobacterial activity or mycolic acid inhibition was reported in the provided publication [76].

## Aromatic type II polyketide

### *Kebanmycins*

Kebanmycins A–D were obtained from *Streptomyces* sp. SCSIO 40068, a mangrove-derived actinomycete discovered by bioactivity-guided fractionation rather than genome mining [77]. The strain was isolated from mangrove rhizosphere sediment and exhibited strong antibacterial activity. The compounds were obtained directly from the native producer with no heterologous expression reported. Kebanmycins A–C possess a fused pyranonaphthaxanthene core with a 6/6/6/6/6/6 polycyclic motif instead of a simple benz[a]anthracene scaffold. The structures were determined from extensive spectroscopic data and single-crystal X-ray diffraction analysis. The biosynthesis gene cluster (*keb*) was identified in the producing strain, and KebMT2 was biochemically characterized as a tailoring sugar-O-methyltransferase. Kebanmycins showed bioactivity against a series of Gram-positive bacteria including *Staphylococcus aureus* and MRSA, and the MIC values of kebanmycin A were 0.125–0.5 μg/mL. They also demonstrated cytotoxicity against several human tumor cell lines. The publication did not contain any specific structure-activity relationship data on the necessity of deoxysugar for antibacterial action [77].

### *WS-5995 A-E*

WS-5995 A–E were isolated from a sea anemone-associated *Streptomyces* sp. S1502 by a genome mining strategy based on metabolic blockade [78]. The wild-type strain was previously described to produce antibacterial streptopyrroles with anti-MRSA activity. Deletion of the core gene *stp1*, encoding an AMP-dependent ligase for the first biosynthetic step of streptopyrroles, resulted in a mutant (S1502/Δ*stp1*) that rerouted the metabolic flow to WS-5995 A–E. WS-5995 E is a novel compound among these. These are unusual angucyclines with an angular tetracyclic benz[a]anthracene skeleton. A biosynthetic gene cluster (*wsm*) was identified by gene knock-out and heterologous expression studies in *Streptomyces lividans* SBT5. Biosynthetic pathways were proposed, and the role of tailoring and regulatory genes was investigated. WS-5995 A showed potent activity against *Eimeria tenella* ($IC_{50}$ = 2.21 μM) and might be an anticoccidial agent. Cytotoxic activities were also tested. In the publication provided, no activity was reported against *Clostridium difficile* or inhibition of toxin production. The compounds may play a protective role in the symbiosis of the bacterium and its sea anemone host [78].

## Polyenes and macrolides

### *Mandimycin*

Instead of traditional genome mining, Mandimycin was discovered by a phylogeny-guided natural-product discovery strategy [21]. Researchers compiled 316,123 bacterial genomes and constructed a phylogenetic tree of mycosamine-transferring glycosyltransferases. The *mand* BGC was identified from *Streptomyces netropsis* DSM 40259 as an orphan clade. Mandimycin is a 38-membered pentaene macrolide (not a heptaene) glycosylated with three deoxy sugars: mycosamine at C-19 and a rare dideoxysaccharide, atratcynose A, at C-35, making it the most heavily glycosylated polyene macrolide reported. Known polyene macrolides recognize ergosterol, but mandimycin has a different target: a spectrum of phospholipids in the fungal cell membrane. It demonstrated potent broad-spectrum fungicidal activity against multidrug-resistant fungal pathogens including *Candida auris*. Mandimycin demonstrated greatly enhanced aqueous solubility (~8.07 mg/mL), over 9,700-fold higher than amphotericin B, and reduced nephrotoxicity. The specific MIC value for *Aspergillus* or *Cryptococcus*, Kd for phosphatidylserine binding, and 4-log CFU reduction data were not shown in the provided publication [21].

### *Spinactinins*

Profiling the biosynthetic enzymes involved in NRP cyclization led to the isolation of spinactins A–E from *Saccharopolyspora spinosa* NRRL 18395 [79]. The work concerned a unique thioesterase, SncF, for δ-lactam formation and expanded the catalytic repertoire of NRPS cyclization domains to include not only the known macrolactam, β-lactam, and γ-lactam types but also δ-lactam. Spinactins are δ-lactam-containing non-ribosomal peptides, but not 22-membered macrolides. The δ-lactam is generated by the TE enzyme SncF, not by an amidotransferase. Spinactin A was less toxic and had higher iron-reducing activity than FDA-approved iron chelators, deferiprone and deferoxamine. This suggests the potential of spinactin A in the treatment of iron overload disorders, especially in β-propeller protein-associated neurodegeneration cells [79].

### *Harundomycin A*

Harundomycin A was discovered from a co-culture of *Streptomyces hygroscopicus* HOK021 and *Tsukamurella pulmonis* TP-B0596 [20,80]. Metabolites produced only in co-culture were revealed by comparative metabolomics and molecular networking using UPLC-QTOF-MS/MS. Harundomycin A is a conjugate of platensimycin (the 2,4-dihydroxy-3-aminobenzoate part of platensimycin) and the catechol-type siderophore N, N'-bis(2,3-dihydroxybenzoyl)-O-seryl-cysteine (bisDHBA-Ser-Cys) connected by a thioester bond. Genomic analysis of S. hygroscopicus HOK021 showed the presence of BGCs for platensimycin and enterobactin, illustrating that *T. pulmonis* serves as an inducer for both pathways. Platensimycin showed comparable antibacterial activity against MRSA and VRE as harundomycin A, and modification with bulky bisDHBA-Ser-Cys did not change the activity. Ferric iron chelating activity comparable to enterobactin was observed by chrome azurol S assays. The compound is a bifunctional molecule for FabF inhibition and siderophore-mediated iron chelation [20].

## Terpenes and terpenoids

### Gromomycins

Gromomycins are a new group of pentacyclic triterpene antibiotics with a cyclic guanidino group forming the fifth six-membered ring, isolated from actinobacteria [81]. The BGC was identified by transposon mutagenesis due to its inability to be assigned by any available bioinformatic tools, which highlights its unique biosynthetic route. Gromomycins are the first bacterial triterpenes synthesized independently of the squalene pathway, employing a hexaprenylguanidine linear precursor and an unprecedented cyclization route. They have strong activity against drug-resistant Gram-positive pathogens, including methicillin- and daptomycin-resistant *S. aureus*. Genome mining uncovered a gromomycin-like biosynthetic gene cluster in the genus *Actinoplanes*, resulting in the isolation of novel bioactive derivatives active against vancomycin-resistant *Enterococci*. Mechanistic studies showed that gromomycins induce rapid leakage of potassium ions and depolarization of the membrane, resulting in the formation of large pores, leakage of intracellular contents, and cell lysis. Supplementation with membrane lipids abolished their activity, confirming direct membrane targeting [81].

### Euthailols

Euthailols are new members of the trans-eunicellane family of diterpenoids identified by functional characterization of an actinobacterial terpene BGC with an unusual architecture [82]. The BGC encodes a terpene cyclase fused to a truncated reductase domain and a cytochrome P450 split into three gene fragments. Heterologous expression in a heterologous host revealed several euthailols with unique oxidation patterns. A pathway-encoded hypothetical protein was identified to have dual isomerase and oxygenase activity. A P450 hydroxylates the eunicellane scaffold at a position that is not modified in other eunicellanes. Both changes showed partial redundancy. Bioactivity assays indicated that some of the euthailols possess growth inhibitory activity against Gram-negative ESKAPE pathogens. No data were reported on anti-inflammatory activity, TNF-α inhibition, or NF-κB suppression. The study highlights that hypothetical proteins are an underexplored family of tailoring enzymes in the biosynthesis of complex terpenoids [82].

### Atralabdans

Heterologous expression of the atr terpenoid gene cluster from *Streptomyces atratus* Gö66 in *Streptomyces albus* J1074 led to the identification of three new labdane diterpenoids with a novel 6/6/5-fused tricyclic skeleton, atralabdans A–C, and the known labdanmycin A [83]. Structures were elucidated by extensive spectroscopic analysis including NMR calculations with DP4+ probability analysis and comparison of experimental and theoretical ECD spectra. Atralabdans A–C showed activity against human neurotropic coxsackievirus B3 (CVB3) but not influenza virus. Compound A was the most potent and had a better therapeutic index than the positive control ribavirin [83].

### Giantene

Giantene was discovered from a giant virus (family Mimiviridae) by characterization of an orphan gene encoding a novel class of terpene synthase, named GV-type terpene synthase [84]. The enzyme GiaTPS was able to use (2E,6E,10E)-geranylgeranyl diphosphate (GGPP) as a substrate to produce a new cyclized terpene compound. The amino acid sequence and the protein structure of this terpene synthase are different from those of the previously known terpene synthases [84].

### Polytolypin

A coworker of Li et al. identified the biosynthetic gene cluster of polytolypin, a potent antifungal, fernane-type triterpenoid, and elucidated its pathway through heterologous expression in *Aspergillus oryzae* NSAR1. The pathway includes a novel triterpene cyclase for motiol biosynthesis, followed by multiple oxidations by three P450s. We characterized two novel triterpene cyclases for isomotiol and fernenol biosynthesis and co-expressed them with the three P450 enzymes, resulting in 13 fernane-type triterpenoids including eight new compounds. Two new compounds showed higher antifungal activity against *Candida albicans* FIM709 than polytolypin. Data were not available for *Cryptococcus neoformans*. This is the first characterization of the biosynthesis of fungal-derived fernane-type triterpenoid [85].

## Metallophores and siderophores

### Cyanochelin B

Cyanochelin B was isolated from the filamentous cyanobacterium *Leptolyngbya* sp. NIES-3755, and not from a Cyanothece species [86]. Its structure was determined by NMR, HRMS, bioinformatic analyses, Marfey's and Murata's methods. Cyanochelin B is a siderophore that chelates iron through two β-hydroxy-aspartate (β-OH-Asp) residues instead of three hydroxamate groups. It is biosynthesized by a hybrid PKS/NRPS gene cluster on plasmid 2 of the producer. The siderophore-$Fe^{3+}$ photolyzes rapidly in the presence of UV-A light with concomitant reduction of $Fe^{3+}$ to $Fe^{2+}$. In coculture experiments, cyanochelin B monopolizes iron for its producer in darkness, whereas UV light abolishes this monopolization and makes iron available for the whole irradiated community [86].

### Lusichelins

Lusichelins A–E were isolated from the marine cyanobacterium *Lusitaniella coriacea* LEGE 07167, not by heterologous expression [87]. These compounds have a unique architecture in which the thiazoline/thiazole rings are connected by a vinyl group, an aliphatic carbon chain, or directly, rather than by hydroxamate groups. We identified a hybrid PKS/NRPS biosynthetic gene cluster (lus). Lusichelins chelate both iron and copper, with lusichelin C always binding iron regardless of the metal condition and copper complexation only observed under high copper conditions. Metal-rich conditions were found to produce the maximum. Lusichelin B exhibited cytotoxic activity against colon carcinoma cells and reversed multidrug resistance by modulation of the ABCB1 efflux pump [87].

### Nitrilobacillins

Nitrilobacillins are a new class of RiPPs with a unique C-terminal nitrile group and not hydroxamate-group siderophores [88]. An asparagine synthetase-like protein converts the carboxylate at the C-terminus of the precursor peptide to a nitrile. An MNIO enzyme catalyzes

stereoselective β-hydroxylation of aspartate and an αKG-HExxH enzyme catalyzes stereoselective β-hydroxylation of proline. The result is a cysteine protease inhibitor with a nitrile warhead, like synthetic protease inhibitors such as the active ingredient in Paxlovid [88].

### Kineochelins

Kineochelins were discovered from *Actinokineospora* sp. UV203, a potentially new species isolated from Antarctic soil, not from *Kineococcus* species [89]. NMR and Marfey's analysis elucidated the structures of kineochelin A1 and E1, which are not three hydroxamate groups but a mixed-ligand structure containing a 2-(2-hydroxyphenyl)-5-methyl-4,5-dihydrooxazole-4-carbonyl subunit. The major congener contains N5-hydroxy-N5-formyl-ornithine, glycine, serine, and a cyclic N5-hydroxy-ornithine terminus. A dedicated NRPS BGC (kin) was found. Kineochelins are potent and selective iron chelators with growth inhibition of Antarctic environmental isolates and selective activity against *Nakaseomyces glabratus* [89].

### Bulbichelin

Bulbichelin was discovered from *Microbulbifer* spp. by a comprehensive mass spectrometry-based workflow with a MassQL code, not by traditional co-culture activation of a silent BGC [19]. We also identified a suite of previously unreported petrobactins with unprecedented longer-chain-length acylation. Biosynthetic pathways were identified by genome mining. Metal infusion mass spectrometry showed that bulbichelins bind a range of metals. Interestingly, no bulbichelins or petrobactins were produced in co-culture with the coral pathogen *Vibrio coralliilyticus*, indicating that Microbulbifer utilizes other strategies such as siderophore piracy. This is the first report of siderophores in the genus Microbulbifer. No catecholate structure was reported, nor any data concerning specific affinity for iron [19].

### Bufferins

Bufferins are the largest family of RiPPs modified by MNIO (DUF692) enzymes, and thousands of homologous BGCs are found throughout the bacterial phylogenetic tree [90]. In the model organism *Caulobacter vibrioides*, conserved cysteine residues in precursor peptides are converted to 5-thiooxazole heterocycles by the concerted action of an MNIO enzyme and a DUF2063 partner protein. Bufferin precursors contain rare N-terminal Sec signal peptides used for export through the Sec pathway. Bufferins do not participate in zinc binding but in copper homeostasis. They enhance bacterial growth under copper stress by complexing excess metal ions in the periplasm. The thiooxazole modifications are required for metal binding. The modification was unambiguously confirmed to be 5-thiooxazoles by selective isotope labeling with 15N and cysteine-specific carbonyl 13C labeling [91]. No Kd values in the range of $10^{-10}$–$10^{-12}$ M or zinc binding were reported [90].

### Cobaltribin

Cobaltribin was not discovered by searching for cobalt-binding BGCs, but rather by high-throughput screening of 500 microbial extracts for inhibitors of the coronavirus main protease 3CLpro [92]. It is the only known isolated natural product containing cobalt, except for the vitamin B12 cobalamins. Bioinformatic, isotope labeling, and gene deletion analyses supported evidence of cobaltribin as a tribrid natural product of an unprecedented terpene-polyketide-nonribosomal peptide trihybridized biosynthetic pathway. Cobaltribin inhibits replication of live SARS-CoV-2 in infected Vero E6 cells without host toxicity [92].

### Methylolanthanin

Methylolanthanin is the first identified physiologically relevant lanthanide-binding metallophore (lanthanophore) produced by the methylotrophic bacterium *Methylobacterium extorquens* AM1 [93]. It features a unique 4-hydroxybenzoate structure not reported for other metallohores. RNA-seq transcriptomics showed 32-fold upregulation of the biosynthetic gene cluster (mll) in cells grown in poorly soluble neodymium (III) oxide versus soluble neodymium (III) chloride. Production of methylolanthanin is required for wild-type levels of cellular lanthanides because deletion of biosynthetic genes causes severe defects in Ln bioaccumulation and overexpression leads to increased bioaccumulation and adsorption. Methylolanthanin was synthesized in total

and can be used for detailed binding studies [94]. Methylolanthanin unexpectedly precipitates with lanthanides under biologically relevant conditions; the solubility product of the Eu3+-MLL complex was found to be -12.07±0.24 mol2 L-2. Methylolanthanin has only a low affinity for $Fe^{3+}$ and differs in this respect from typical siderophores. Accumulation of Nd and secretion of MLL are significantly increased under Fe-limiting conditions. These findings suggest a complex relationship between iron and lanthanide metabolism inLn-using bacteria [93,94].

## Cyanobacterial natural products

Cyanobacteria remain a prolific source of structurally diverse and biologically active compounds.

### Monchicamides A–K

Eleven novel macrocyclic cyanobactins, monchicamides A–K, were identified from the *Microcoleaceae cyanobacterium* LEGE 16532 via genome mining [95]. The mon BGC (11.2 kb) encodes five precursor peptides with 8–11 amino acid core sequences and typical cyanobactin biosynthetic genes, including a protease, macrocyclase, and a prenyltransferase (MonF). The monchicamides are macrocyclic derivatives with monoprenylated, diprenylated, and nonprenylated variations. Monchicamide I was isolated, and its structure was confirmed by NMR and MS/MS, establishing forward O-prenylation on tyrosine. Marfey's analysis showed that all amino acids were in the L-configuration. Monchicamide G is the first reported cyanobactin with prenyl groups on two tyrosine residues that are catalyzed by a single prenyltransferase. Monchicamide I showed no cytotoxic, antimicrobial, or antiamoebic activity. This work expands the chemical diversity of the cyanobactin family and points to the biosynthetic potential of under-investigated cyanobacterial taxa [95].

### Hyellamide

*Hyella patelloides* LEGE 07179, a pleurocapsalean cyanobacterium, was subjected to bioactivity-guided fractionation, resulting in the isolation of hyellamide, a glycosylated N-acyl tyrosine-derived eneamide [96]. Its structure was elucidated as a 4-[(E)-2-aminovinyl] phenol core N-acylated with tetradecanoic acid and bearing a β-D-4-O-acetyl-xylopyranose fragment by NMR and HRESIMS/MS. This is the second class of secondary metabolites reported from the order Pleurocapsales. The predicted hyell BGC encodes a flavin-dependent oxidase (HyeB), acyltransferase (HyeC), glycosyltransferase (HyeH), and acetyltransferase (HyeG). The isolation was guided by the initial antimicrobial activity. Pure hyellamide did not inhibit *Bacillus subtilis*, indicating that the activity was due to a co-eluting polyunsaturated fatty acid. This is the first N-acylated tyrosine eneamide reported from cyanobacteria, expanding the chemical repertoire of this underexplored taxonomic order [96].

### Fatuamide A

Fatuamide A was isolated from a marine *Leptolyngbya* sp. collected in American Samoa by bioassay-guided fractionation against NCI-H460 lung cancer cells [97]. The linear hybrid PKS/NRPS architecture resolved by NMR and MS/MS contains a salicylate-derived thiazoline, two phenylalanine residues, and terminal glycine. Absolute configuration at eight stereocenters was determined using bioinformatic and computational methods such as DP4+ analyses. The structure fitted a tentative hybrid PKS/NRPS BGC. Native metabolomics revealed fatuamide A to be a metallophore with a preference for copper binding. The producing strain displayed an extraordinary copper tolerance (>1,000-fold above natural seawater concentrations). This is only the third phenolate-type siderophore from cyanobacteria. Although pure fatuamide A showed no activity against the NCI-H460 cells from which it was isolated, from the most cytotoxic fraction, it was suggested that another minor component was responsible [97].

### Cyanopeptolin analogues and Suomilide F

The investigation of *Nostoc* sp. UIC 10890 with 15N stable isotope labeling in combination with genome mining resulted in the discovery of three novel compounds and revealed five groups of nitrogen-containing metabolites [18]. AntiSMASH analysis revealed 27 BGCs, of which 11 were predicted to encode nitrogen-containing products. Suomilide F, a novel aeruginosin-like compound containing an azabicyclononane moiety and an α-galactose unit, as opposed to the α-

glucose in the previously reported suomilides. Its BGC was aligned to known suomilide clusters, but the glycosyltransferase had only 0.8% sequence identity. Leucine or tyrosine in position 2 and butanoic or hexanoic acid side chains were found in two new cyanopeptolin analogues, UIC949 and UIC999. All three compounds inhibit serine proteases such as trypsin, chymotrypsin, and elastase. This study demonstrates the power of combining isotopic labeling and genome mining to link metabolites to their BGCs in cyanobacteria [18].

### Brominated indole biosynthetic machinery

Researchers used metagenomic analysis to identify two new cyanobacterial haloindole BGCs from marine sediment in Moorea and soil-derived samples in Hawaii, targeting two previously uncharacterized enzymes involved in aetokthonotoxin biosynthesis—tryptophan halogenase AetF and nitrile synthase AetD [98]. The authors had recently characterized the functions of these two enzymes that had been annotated as hypothetical proteins. A new AetF homologue was biochemically validated and was found to exclusively halogenate free indole rather than tryptophan as in AETX biosynthesis, thus expanding the known substrate scope. This new AetD homologue, which has different substrate preferences, expanded the scope of nitrile biosynthesis. Characterization of core and accessory enzymes within these AETX-like BGCs underscored the breadth and diversity of the haloindole biosynthetic machinery in cyanobacteria. Here, we demonstrate that sequence-divergent biosynthetic enzymes can be effective probes for metagenomic discovery of new biosynthetic pathways [98].

### Metagenomic assessment of a *Dolichospermum* bloom

An extensive shotgun metagenomic analysis of a surface bloom of *Dolichospermum lemmermannii* from Lake Garda, Italy in summer 2020 led to an almost complete metagenome-assembled genome [99]. The phylogenomic analysis clarified the taxonomic position of this species in the ADA (*Anabaena*/*Dolichospermum*/*Aphanizomenon*) clade. The genome annotation revealed unique adaptive features allowing bloom formation in oligotrophic lakes, including nitrogen fixation capabilities. We identified BGCs encoding geosmin, anabaenopetins, and other bioactive compounds. LC-MS/MS analysis of cyanotoxins revealed no presence of Microcystins, anatoxins, cylindrospermopsin, and saxitoxins. Functional annotation shed light on central metabolism and competitive traits underlying cyanobacterial blooms. The present study shows how metagenomic approaches can be useful to comprehensively characterize cyanobacterial bloom events and their potential for secondary metabolite production [99].

## Marine compounds derived from unique ecosystems

Extreme marine environments such as deep-sea sediments, Antarctic waters, and sponge-associated microbes have given rise to compounds with remarkable structural diversity and excellent biological activities, as shown in **Figure 2**.

### Antarmycins

Antarmycin A was obtained from the deep-sea-derived rare actinomycete *Pseudonocardia antarctica* SCSIO 07407 (sediment at the depth of 3,386 m) using bioassay-guided fractionation targeting VRE and MRSA [100]. It features a symmetric 16-membered macrodiolide core with two pendant vancosamine groups, one glucosylated, the first report of vancosamine in macrodiolide natural products. The *ant* BGC was located on a giant conjugative plasmid (pAn001, 352.7 kb) containing multiple transferable elements. Seven genes were associated with vancosamine biosynthesis, and two glycosyltransferases (AntC and AntD) were characterized. Antarmycin A exhibited potent activity against MDR *E. faecium* (MIC 0.25–1 μg/mL) and MRSA (MIC 1–4 μg/mL) with rapid bactericidal activity and showed efficacy in in vivo models of intestinal and epicutaneous infection. Mechanistic studies revealed membrane disruption by vancosamine interaction with phosphatidylglycerol/phosphatidylethanolamine. The structure–activity relationship studies confirmed the importance of the vancosamine for the antibacterial activity [100].

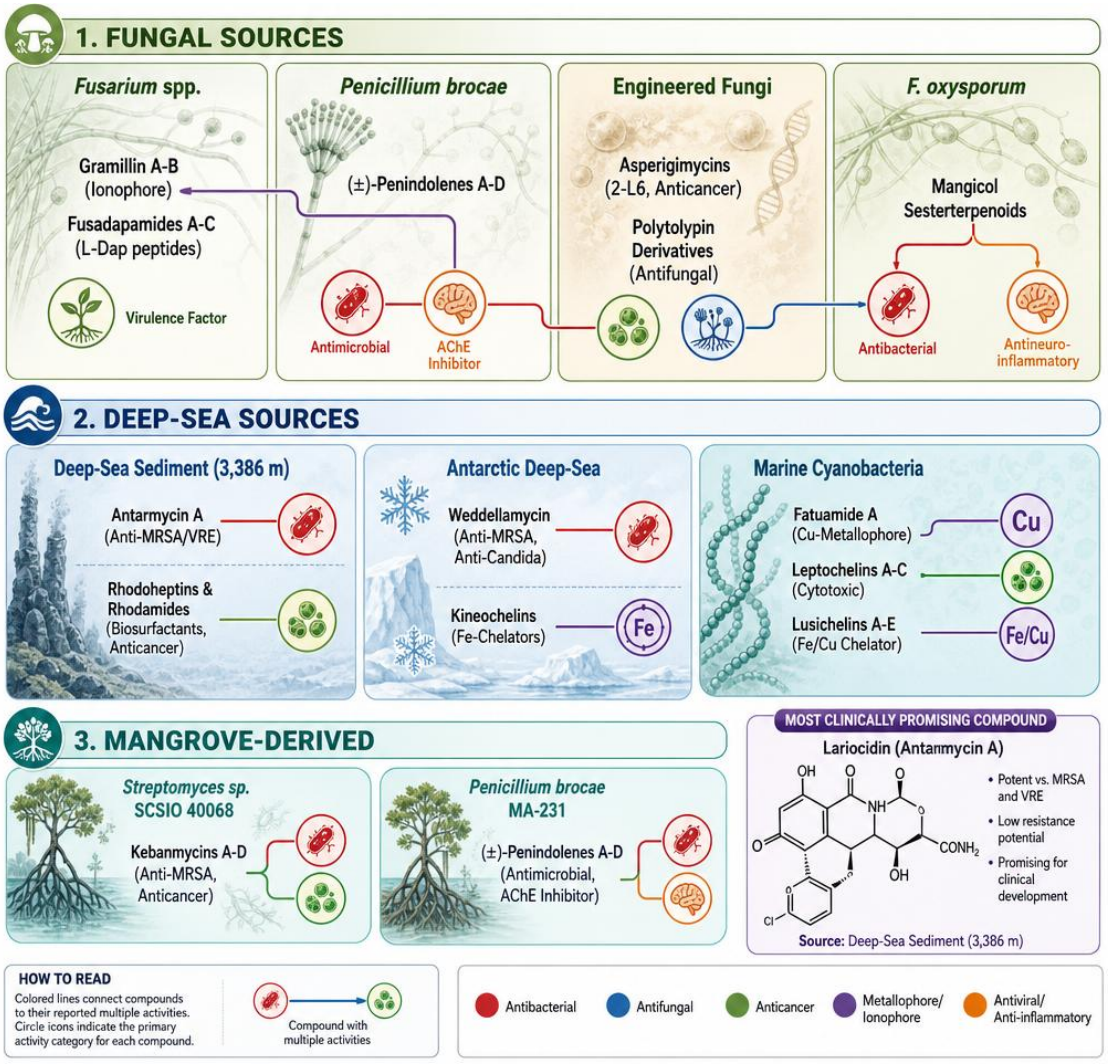


Figure 2. Fungal and deep-sea microbial natural products (2023–2026). Compounds are organized by ecological source across three categories with activity color coding: red (antibacterial), blue (antifungal), green (anticancer), purple (metallophore/ionophore), and orange (antiviral/anti-inflammatory).

## Rhodoheptins and rhodamides

Genome mining of the deep-sea actinobacterium *Rhodococcus* sp. I2R combined with MS-based metabolomics led to the identification of 20 new cyclolipopeptides (rhodoheptins) and 33 new glycolipopeptides (rhodamides) [101]. Rhodoheptins are cyclic heptapeptides conjugated at the N-terminus to β-hydroxy fatty acids (C16–C24), and the macrolactone ring is formed by cyclization catalyzed by thioesterase. Rhodamides are linear 14-mer glycolipopeptides with serine- and alanine-rich backbones with characteristic acetylation, glycosylation, and succinylation. Structures were assigned by combining in silico BGC analysis with HRMS/MS data, as the production levels were too low for NMR. Five NRPS gene clusters with starter condensation domains were identified, and two of these LP families were associated with these. Both classes of compounds showed biosurfactant activity in oil-spreading assays and moderate antiproliferative activity against human A375 melanoma cells. This study shows the potential of deep-sea *Rhodococcus* for the discovery of biosurfactants [101].

## Weddellamycin from antarctic deep-sea *Streptomyces* sp. DSS69

Chen and co-workers identified weddellamycin, a polyene macrolactam with a unique 23/5/6 ring skeleton from the sponge-associated Antarctic deep-sea bacterium *Streptomyces* sp [102]. DSS69 was identified through genome mining and heterologous expression. Cloning and expression of cryptic BGC for compound discovery. Regulatory studies revealed a negative

regulator (WdlO) and two positive regulators (WdlA and WdlB). Overexpression of *wdlA* and *wdlB* along with deletion of *wdlO* resulted in greatly increased fermentation titers. Weddellamycin displayed potent antibacterial activity against Gram-positive bacteria including MRSA (MIC 0.10–0.83 μg/mL) and antifungal activity against *Candida albicans* (MIC 3.33 μg/mL). The compound was also cytotoxic to several cancer cell lines with IC50 values of 2.07–11.50 μM. The study reveals the potential of integrating genome mining and heterologous expression to access cryptic biosynthetic pathways from underexplored Antarctic deep-sea actinomycetes [102].

### Dactylides D and E of *Dactylosporangium aurantiacum*

*Dactylosporangium aurantiacum* ATCC 23491 yielded two new 22-membered polyol macrolides, dactylide D (1) and dactylide E (2), and the known dactylosporolide B [103]. Compound 1 has an N-acetylalanyl side chain, and compound 2 has an unusual (E)-7-amino-oxohept-5-enoic acid moiety with oxidation at the C-7 position and loss of the tetrahydropyran ring characteristic of earlier dactylides. NOE correlations confirmed the stereochemistry of the macrolactone core to be the same as dactylide B. These changes represent major structural modifications in the family of dactylides, which was already expanded in 2023 by the same group with dactylides A-C. Closely related compounds, dactylosporolides, are glycosylated macrolides recently characterized from *Dactylosporangium fulvum*. The dactylides belong to a growing family of polyol-type 22-membered macrolides. These findings increase the structural diversity of polyol macrolides from *D. aurantiacum*, highlighting the continued natural product discovery potential of this strain [103].

## Natural products of fungi

New chemical scaffolds are still being discovered from fungi, particularly from underexplored lineages and ecological niches.

### Gramillin A and B

Gramillin A and B are bicyclic lipopeptides that were isolated from *Fusarium graminearum* and identified as products of the NRPS8 gene cluster [104]. The fused bicyclic structure is formed by macrocycle closure with a rare anhydride bond. Disruption of the *GRA1* biosynthetic gene and transcription factor *GRA2* was analyzed. Gramillins are produced in planta on maize silks and increase virulence on maize but not on wheat, thus showing host-specific adaptation. Gramillin acts as a cation-selective ionophore, creating pores in the lipid bilayers leading to plasma membrane depolarization, ion leakage into the apoplast, and necrosis [105]. ROS induced by Gramillin requires host genes *ILK1*, *RBOHD*, and *BIK1*. Activity was lost on linearization or disulfide reduction, confirming the requirement for the cyclic structure. The results establish that the ionophore activity of gramillin is one of the mechanisms that target plant membranes and coordinate fungal pathogenesis [104,105].

### Asperigimycins

Aspergimycins are a distinct family of fungal RiPPs with a heptacyclic scaffold consisting of a benzofuranoindoline core and three additional macrocycles, generated by six fungi-specific DUF3328 oxidases [106]. The N-terminal pyroglutamate improves the anticancer activity of asperigimycins C and D. Inactive asperigimycin B was chemically modified with lipid substitution to generate a C-11 fatty acid derivative (2-L6) with nanomolar potency comparable to that of marketed antileukemia drugs. CRISPR screening identified the SLC46A3 transporter as essential for 2-L6 cellular uptake. This work reveals the untapped therapeutic potential of fungal RiPPs relative to their bacterial counterparts and illustrates lipid modifications for engineering asperigimycins as anticancer leads. The unprecedented architecture broadens the knowledge of fungal RiPP biosynthetic complexity [106].

### Fusadaparides

Fusadapamides A–C are new linear tripeptides from fungi of *Fusarium poae* with L-2,3-diaminopropionic acid (L-Dap) [107]. The BGC was identified using untargeted metabolomics and long-read sequencing and is located on an accessory chromosome, representing the first

telomere-to-telomere assembly for this species. The trimodular NRPS Fda1 carries a unique terminal condensation domain that is phylogenetically distinct from cyclization domains. Fda4 condenses O-phosphoserine with L-alanine, and Fda3, a FAD-dependent oxidoreductase, completes the pathway, which differs from bacterial and plant systems. L-Dap biosynthesis occurs via a two-gene module. Homologous dap modules involved in fusadapamide biosynthesis are present in diverse ascomycetes, but fusadapamide production is rare in *Fusarium* (~6.5% of strains). This study illustrates how population-scale metabolomics can uncover biosynthetic innovations linked to accessory chromosomes [107].

### (±)-Penindolenes A–D

The mangrove fungus *Penicillium brocae* MA-231 [104,108] afforded (±)-Penindolenes A–D, the first indole terpenoids with a γ-lactam skeleton. The pathway was elucidated by heterologous expression and in vitro assays, identifying five enzymes (PbaABCDE). The first example of oxidative indole cleavage by a P450 monooxygenase, P450 monooxygenase PbaB, catalyzed the 2,3-cleavage of the indole ring. A rare secondary amide bond is catalyzed by a glutamine synthetase-like enzyme, PbaD. Enantiomer 2a demonstrated high activity against aquatic pathogens (MIC 0.5–16 μg/mL). Compound 1a showed good acetylcholinesterase inhibition with an IC50 of 0.098 μM, which was better than the positive control, tacrine. Racemic mixtures were less active than pure enantiomers. These findings broaden enzymatic indole chemistry and offer bioactive leads for pharmaceutical development [104,108].

## Modern tools and biosynthetic enzymology

The years 2023–2026 provided important insights into the enzymatic mechanisms and modern discovery platforms that drive natural product biosynthesis, as shown in **Table 1**.

### Mechanistic enzymology

Several papers described new enzymatic transformations. The cytochrome P450 monooxygenase PbaB from *Penicillium brocae* catalyzes oxidative indole cleavage by a P450 to generate two keto groups via 2,3-cleavage of the indole ring, the first example of oxidative indole cleavage by a P450 [108]. This broadens the known catalytic range of P450 enzymes beyond hydroxylation and epoxidation.

Unexpected chemistry continues to be revealed in MNIO (DUF692) enzymes of RiPP biosynthesis. Conversion of cysteine residues into 5-thiooxazole heterocycles by an MNIO enzyme and a DUF2063 partner protein in the bufferin biosynthesis [90]. This modification was unequivocally confirmed by selective isotope labeling with $^{15}N$ and cysteine-specific carbonyl $^{13}C$ labeling [91]. In nitrilobacillin biosynthesis, an asparagine synthetase-like protein converts a C-terminal carboxylate to a nitrile, an unprecedented modification in RiPPs, while an MNIO enzyme and an αKG-HExxH enzyme stereoselectively β-hydroxylate aspartate and proline, respectively [88].

The thioesterase SncF from *Saccharopolyspora spinosa*, which forms a δ-lactam, broadens the catalytic capabilities of NRPS cyclization domains beyond macrolactam, β-lactam, and γ-lactam types [79]. The biosynthesis of pyridomycin involves a coordinated NRPS-PKS hybrid system that catalyzes the formation of 3-(3-pyridyl)-L-alanine. The type I PKS enzyme Pyr9 condenses nicotinic acid and 1,3-bisphosphoglycerate [70].

The lasso peptide field discovered the prenyltransferase MonF, which can install prenyl groups on two tyrosine residues within a single cyanobactin, a first for this class of enzyme [95]. The lasso peptide biosynthetic landscape was further expanded by the discovery of split-operon architecture in cebulassopin biosynthesis, where precursor and maturation genes are encoded megabase pairs [30], and an AraC-precursor fusion protein regulating actinosynnelassin production [31].

In the context of graspetide biosynthesis, the ATP-grasp enzyme ThfB was shown to catalyze the formation of ester linkages as well as thioester cross-links, offering a recombinant pathway to head-to-tail cyclic peptides via native chemical ligation [39]. Partner-dependent biosynthesis of rosaritide and corallotide is a novel regulatory mechanism in which cognate partner proteins are required for graspetide synthetase activity [41].

### Discovery platforms in the modern era

There were also several new discovery platforms that emerged in this period. By using the 15N stable isotope labeling approach in combination with genome mining, we linked nitrogen-containing metabolites to their corresponding BGCs in *Nostoc* sp. and discovered suomilide F and cyanopeptolin analogs [18]. This method takes advantage of the ability of cyanobacteria to incorporate inorganic nitrogen into secondary metabolites.

Using phylogeny to guide the discovery of natural products, mandimycin was discovered by building a phylogenetic tree of 316,123 bacterial genomes that contained mycosamine-transferring glycosyltransferases [21]. This approach leverages evolutionary divergence of conserved biosynthetic enzymes to identify metabolites with novel modes of action.

The MassQL (mass spectrometry-based query language) workflow allowed the discovery of bulbichelin and new petrobactins from *Microbulbifer* spp., providing a reproducible method for metallophore discovery that could be used for any organism [19]. Combined culture metabolomics and molecular networking revealed that harundomycin A is a bifunctional conjugate produced only in co-culture of *Streptomyces hygroscopicus* and *Tsukamurella pulmonis* [20].

The synthetic-bioinformatic natural product (syn-BNP) approach uses high-accuracy structure prediction and chemical synthesis to quickly access predicted products from silent or inaccessible BGCs for discovery of chisopeptins [15]. This strategy avoids the problems of heterologous expression or cultivation of native producers.

CFPS enabled the production of embleporicin, the first class I lanthipeptide produced from actinobacteria by this method, suggesting the potential of CFPS for accessing RiPPs from genetically difficult organisms [36].

Population-scale untargeted metabolomics coupled with long-read genome sequencing identified the fusadapamide BGC on an accessory chromosome in *Fusarium poae*, highlighting the power of integrating chemical and genomic data across populations to discover biosynthetic innovations [107].

The employed genetic manipulation strategies included promoter engineering to deregulate silent BGCs (biffamycin A) [7], deletion of global regulators to activate cryptic pathways (olikomycin A by wblA deletion) [6], and metabolic blockade-based genome mining where deletion of a competing pathway diverts metabolic flux (WS-5995 A–E by stp1 deletion) [78].

## Clinical and agricultural relevance

The compounds identified in the period 2023 to 2026 exhibit remarkable biological activity with important implications in therapeutics and agriculture, as shown in **Table 1**.

### Antibiotic against drug-resistant bacteria

Several compounds show promise in treating multi-drug-resistant infections. Lariocidin, a lasso peptide from *Paenibacillus* sp. M2 is active against Gram-positive and Gram-negative pathogens with broad-spectrum activity via targeting a novel ribosomal binding pocket which is distinct from all known antibiotic sites [26]. Importantly, it shows in vivo efficacy in a mouse *Acinetobacter baumannii* infection model and a low propensity for the development of spontaneous resistance. Its self-resistance mechanism via the N-acetyltransferase LrcE, whose homologs are largely absent from clinical pathogens, further supports development potential [29]. Antarmycin A, isolated from deep-sea *Pseudonocardia antarctica*, showed strong activity against MDR *E. faecium* (MIC 0.25–1 μg/mL) and MRSA (MIC 1–4 μg/mL) with quick bactericidal effect and in vivo efficacy in both intestinal and epicutaneous infection models [100]. Its unique vancosamine-decorated macrodiolide scaffold interacts with phosphatidylglycerol/phosphatidylethanolamine to target bacterial membranes. Pyridomycin is a unique example of a compound bridging the NADH- and substrate-binding pockets to directly inhibit the enoyl reductase InhA and, importantly, isoniazid-resistant clinical isolates are fully susceptible [68,71]. However, neither pyridomycin nor its analogs were effective in a murine tuberculosis model, although improved semisynthetic derivatives with enhanced metabolic stability were reported [71].

Neosorangicin A, a very potent in vitro inhibitor of bacterial RNA polymerase, shows enhanced activity against MRSA (MIC 0.0625 μg/mL) and *M. tuberculosis* (MIC 1.6 μg/mL) compared to sorangicin A (over 10-fold better) [73]. However, rapid degradation in mouse plasma (half-life <0.5 min) precluded in vivo efficacy, underlining the importance of ADME profiling early in drug development. Corramycin is a zwitterionic modified peptide antibiotic from *Corallococcus coralloides* active against Gram-negative pathogens, with optimized derivatives showing broad-spectrum activity and outstanding efficacy in multiple mouse infection models [53,54]. Griselimycin, a DNA sliding clamp DnaN inhibitor, has potent activity against *M. tuberculosis*, with the cyclohexyl derivative showing a MIC of 0.05 μM [56,57]. Fluorophore-labeled analogues remain active and accumulate in macrophage phagosomes [58].

## Antifungal drugs

Mandimycin is a landmark discovery of an antifungal with potent broad-spectrum fungicidal activity against multidrug-resistant *Candida auris* and other fungal pathogens [21]. It has a unique mode of action by targeting different phospholipids in the cell membrane of fungi rather than ergosterol, with > 9700-fold improved aqueous solubility and decreased nephrotoxicity compared to amphotericin B. Antarctic deep-sea *Streptomyces* sp. DSS69 Weddellamycin exhibited excellent antibacterial activity against MRSA (MIC 0.10–0.83 μg/mL) and antifungal activity against *Candida albicans* (MIC 3.33 μg/mL), and also exhibited additional cytotoxicity against cancer cell lines [102]. Polytolypin, a fernane-type triterpenoid, and its two engineered derivatives exhibited stronger antifungal activity against *C. albicans* than the parent compound, illustrating the potential of combinatorial biosynthesis for antifungal development [85].

## Antiviral drugs

Cobaltribin is the only isolated natural product that contains cobalt, other than vitamin B12 cobalamins, which inhibits the replication of live SARS-CoV-2 in infected Vero E6 cells without host toxicity [92]. The novel terpene-polyketide-nonribosomal peptide tribrid architecture represents a new antiviral scaffold. Among these, the Atralabdans A–C from *Streptomyces atratus* inhibit human neurotropic coxsackievirus B3 (CVB3) with a higher therapeutic index than the positive control ribavirin, especially compound A [83].

## Applications in agriculture

*Fusarium oxysporum* mangicol sesterterpenoids showed antimicrobial activity against plant pathogen *Ralstonia solanacearum* (MIC 6.25–25 μM), indicating potential for crop protection [75]. Gramillin is a cyclic lipopeptide ionophore produced by F*usarium graminearum* that targets plant membranes to enhance fungal virulence, and understanding its mechanism may inform strategies to confer resistance to Fusarium head blight in cereal crops [104,105].

## Possible anticancer

Heptacyclic fungal RiPPs, asperigimycins, were engineered to produce a C-11 fatty acid derivative (2-L6) that exhibits nanomolar anticancer activity comparable to approved antileukemia drugs [106]. Cellular uptake requires the SLC46A3 transporter (identified by CRISPR screening). (±)-Penindolenes A-D, indole terpenoids bearing a γ-lactam skeleton, exhibited potent antimicrobial and acetylcholinesterase inhibitory activities [108]. Enantiomer 1a was superior to tacrine with an $IC_{50}$ value of 0.098 μM. *Saccharopolyspora cebuensis* Cebulassopin A showed selective antiproliferative activity against A549 lung carcinoma cells ($IC_{50}$=0.786 μM) and was more prominent than etoposide [30]. Fatuamide A, a metallophore isolated from marine *Leptolyngbya* sp., and leptochelins A–C, isolated from geographically dispersed Leptothoe strains, were both cytotoxic against cancer cell lines [97,109].

Table 1. Biosynthetic enzymology, modern discovery tools, and therapeutic applications (2023–2026)

| Category | Enzyme/tool/compound | Source/System | Key feature | Relevance/application |
|---|---|---|---|---|
| Novel enzymatic mechanisms | | | | |
| Oxidative indole cleavage | P450 monooxygenase (PbaB) | *Penicillium brocae* MA-231 | First P450-catalyzed 2,3-cleavage of indole ring | Expands P450 catalytic repertoire for biocatalysis |
| δ-Lactam formation | Thioesterase (SncF) | *Saccharopolyspora spinosa* NRRL 18395 | First δ-lactam-forming TE domain | Expands NRPS cyclization beyond macrolactam, β-, γ-lactams |
| C-Terminal nitrile introduction | Asparagine synthetase-like protein | Nitrilobacillin BGC | Unprecedented RiPP modification; protease inhibitor warhead | Analogous to synthetic drugs (e.g., Paxlovid) |
| 5-Thiooxazole formation | MNIO + DUF2063 partner | *Caulobacter vibrioides* (Bufferins) | Cysteine to 5-thiooxazole conversion; Cu homeostasis | Largest RiPP family; confirmed by $^{15}N/^{13}C$ labeling |
| Lanthanophore biosynthesis | Mll BGC (*mllA–mllJ*) | *Methylobacterium extorquens* AM1 | First lanthanide-binding metallophore; 4-hydroxybenzoate moiety | Green lanthanide mining; rare earth recovery |
| L-Dap biosynthesis | Fda4 (PLP-dependent) + Fda3 (FAD-dependent) | *Fusarium poae* Fp133 | First fungal L-Dap pathway; OPS + L-Ala condensation | Distinct from bacterial and plant pathways |
| Viral terpene synthase | GiaTPS (GV-type) | Giant virus (Mimiviridae) | First terpene synthase from a virus; distinct sequence/structure | Expands enzymatic diversity to viral domain |
| Partner-dependent graspetide maturation | MirB + MirC; CorB + CorC | *Micromonospora rosaria*; *Corallococcus exercitus* | Novel regulatory mechanism; partner proteins required for activity | New paradigm in RiPP biosynthesis |
| Split biosynthetic operons | PdmA/PdmB-C; CbpA1/CbpB1 | *Pseudomonas tolaasii*; *Saccharopolyspora cebuensis* | Bipartite BGC architecture; independent regulation | Expands genome mining scope for RiPP discovery |
| Thioester cross-link formation | ATP-grasp enzyme (ThfB) | Pre-fuscimiditide | Enables recombinant head-to-tail cyclic peptides | Tool for protein/peptide cyclization |
| AraC-precursor fusion | AlnR/A regulatory protein | *Actinosynnema pretiosum* | Largest lasso peptide precursor; regulator-peptide fusion | Novel genetic architecture |
| Modern discovery platforms | | | | |
| $^{15}N$ stable isotope labeling | Comparative metabolomics | *Nostoc* sp. UIC 10890 | Directly links metabolites to BGCs via nitrogen counting | Suomilide F + cyanopeptolin discovery |
| Phylogeny-guided discovery | Mycosamine-transferring glycosyltransferase tree | 316,123 bacterial genomes | Leverages evolutionary divergence for novel compounds | Mandimycin discovery |
| MassQL workflow | Programmable mass spectrometry | *Microbulbifer* spp. | Targeted metallophore discovery; replicable for any organism | Bulbichelin + petrobactin discovery |
| Synthetic-bioinformatic (syn-BNP) | Structure prediction + SPPS | *Chitinophaga solisilvae* BGC | Circumvents expression challenges; rapid access to predicted products | Chisopeptin discovery |

| Category | Enzyme/tool/compound | Source/System | Key feature | Relevance/application |
|---|---|---|---|---|
| Combined-culture metabolomics | Co-culture + molecular networking | *Streptomyces* + *Tsukamurella* | Reveals cryptic metabolites induced by microbial interactions | Harundomycin A discovery |
| Cell-free protein synthesis | CFPS + total RNA + $ZnCl_2$ | *Embleya* sp. NF3 | First class I lanthipeptide from actinobacteria by CFPS | Embleporicin production |
| Population-scale metabolomics | Untargeted MS + long-read sequencing | *Fusarium poae* (59 strains) | Links accessory chromosome BGCs to chemical phenotypes | Fusadapamide discovery |
| Metabolic blockade | Competitive pathway deletion (*Δstp1*) | *Streptomyces* sp. S1502 | Redirects metabolic flux to silent BGCs | WS-5995 A–E discovery |
| Therapeutic applications | | | | |
| Antibacterial | Lariocidin, Antarmycin A, Gromomycins, Griselimycin, Corramycin | Various microbial sources | Novel targets (ribosome, membrane, DnaN, InhA, RNAP) | MDR Gram-positive and Gram-negative infections; tuberculosis |
| Antifungal | Mandimycin, Weddellamycin, Polytolypin derivatives | *Streptomyces*, fungal sources | Phospholipid targeting; reduced nephrotoxicity | MDR *Candida auris*; invasive candidiasis |
| Antiviral | Cobaltribin, Atralabdans A–C | Microbial extract; *Streptomyces atratus* | SARS-CoV-2 3CLpro; CVB3 capsid | COVID-19; enteroviral infections |
| Anticancer | Asperigimycins (2-L6), Cebulassopin A, Ajudazols C–H, (±)-Penindolenes | Fungal, actinobacterial sources | Nanomolar potency; selective tumor targeting | Leukemia; lung carcinoma; pancreatic cancer |
| Iron overload | Spinactin A | *Saccharopolyspora spinosa* | Superior iron-reducing vs. deferiprone/deferoxamine | BPAN; thalassemia |
| Metal Homeostasis | Bufferins, Methylolanthanin | *Caulobacter vibrioides*; *M. extorquens* | Copper detoxification; lanthanide recovery | Wilson disease; green mining |
| Agriculture | Gramillin, Mangicols | *Fusarium* spp. | Plant membrane targeting; crop pathogen control | Fusarium head blight; *Ralstonia* wilt |
| Key translational lessons | | | | |
| ADME Importance | Neosorangicin A | *Sorangium cellulosum* | Potent in vitro (MIC 0.0625 μg/mL) but failed in vivo ($t_{1/2}$ <0.5 min) | Early PK profiling essential |
| Semisynthetic optimization | Pyridomycin analogs | *Dactylosporangium fulvum* | Improved metabolic stability but insufficient for in vivo efficacy | Manageable liabilities critical |
| Novel binding modes | Griselimycin (DnaN), Mandimycin (phospholipids) | Microbial sources | Unique target engagement avoids existing resistance | Resistance-evading therapeutics |

### Other therapeutic uses

Spinactin A displayed lower cytotoxicity and better iron-reducing activity compared to the FDA-approved iron chelators deferiprone and deferoxamine, implying its potential in treating iron overload disorders such as BPAN [79]. Bufferins are a widespread copper homeostasis mechanism and may be useful in diseases involving metal misregulation [90]. The first lanthanide-binding metallophore methylolanthanin allows microbial lanthanide mining and points to *Methylobacterium extorquens* as a green chassis for recovering supply-chain-limited rare earth elements [93].

### Mechanistic & translational insights

Several compounds provide important lessons for drug development. Neosorangicin A demonstrated that good in vitro efficacy does not equate to *in vivo* efficacy due to its poor plasma stability [73]. The journey of pyridomycin from natural product to semisynthetic optimization exemplifies the opportunities and difficulties of targeting validated drug targets with novel binding modes [68–71]. Deep-sea sediments, Antarctic waters and other underexplored ecological niches still yield molecules with clinically relevant activities and novel mechanisms as exemplified by mandimycin and antarmycin A [21,100].

## Conclusion

The discovery of microbial natural products with significant therapeutic potential has experienced a remarkable expansion from 2023 to 2026, a phenomenon that has been facilitated by advancements in metabolomics platforms, synthetic biology, and genome mining. Several discoveries are noteworthy for their clinical potential, including the in vivo efficacy of lariocidin against *Acinetobacter baumannii*. Mandimycin demonstrated potent activity against multidrug-resistant *Candida auris* with reduced nephrotoxicity compared with amphotericin B by targeting a novel ribosomal binding pocket. Cobaltribin, the first cobalt-containing tribrid natural product, inhibited SARS-CoV-2 replication. Griselimycin and pyridomycin analogs maintained activity against drug-resistant *Mycobacterium tuberculosis*. Anticancer properties, such as cebulassopin and asperigimycins with nanomolar potency, have been engineered through lipid modification. The comprehensive therapeutic potential of microbial metabolites is further underscored by a selective agent that targets lung carcinoma cells. In addition to individual compounds, our comprehension of natural product assembly has been significantly enhanced by fundamental insights into biosynthetic enzymology, such as oxidative indole cleavage by P450 monooxygenase, δ-lactam formation by thioesterase domains, C-terminal nitrile introduction in RiPPs, 5-thiooxazole formation by MNIO enzymes, split biosynthetic operons, and viral terpene synthases.

However, substantial obstacles persist despite these developments. The significance of early ADME profiling is underscored by the failure of numerous promising compounds to translate in vitro potency to in vivo efficacy, which was attributed to their poor pharmacokinetic properties. The development of improved heterologous expression systems, the application of synthetic biology for yield optimization, the continued exploration of underexplored ecological niches, and the integration of artificial intelligence with genome mining will expedite the translation of microbial natural products into clinically useful therapeutics. The central role of microbial natural products—from bacteria, fungi, cyanobacteria, and even viruses—in addressing urgent therapeutic needs, including multidrug-resistant infections, cancer, and emergent viral diseases, is further emphasized by the compounds and biosynthetic insights described in this review.

### Ethics approval

Not required.

### Acknowledgments

A.F. thanks the Organization for Research and Agriculture -- BRIN.

### Competing interests

All the authors declare that there are no conflicts of interest.

**Funding**

This study received no external funding.

**Underlying data**

No new data are generated in this study.

**Declaration of artificial intelligence use**

Artificial intelligence (AI) AI-based language model, ChatGPT, was employed to language refinement (improving grammar and readability of the manuscript). Authors confirmed that all AI-assisted processes were critically reviewed by the authors to ensure the integrity and reliability of the results. The final decisions and interpretations presented in this article were solely made by the authors.

## How to cite

Frediansyah A, Azzahra FL, Kantisin S, *et al*. Novel antibiotics, antifungals, antivirals, and anticancer agents from microbial sources (2023–2026): Chemistry, biosynthesis, and therapeutic potential. Narra Thera 2026; 1 (1): e4 - http://doi.org/10.52225/narrathera.v1i1.4.

## References

1. Newman DJ, Cragg GM. Natural products as sources of new drugs over the nearly four decades from 01/1981 to 09/2019. J Nat Prod 2020;83(3):770-803.
2. Atanasov AG, Zotchev SB, Dirsch VM, *et al.* Natural products in drug discovery: Advances and opportunities. Nat Rev Drug Discov 2021;20(3):200-216.
3. Navarro-Muñoz JC, Selem-Mojica N, Mullowney MW, *et al.* A computational framework to explore large-scale biosynthetic diversity. Nat Chem Biol 2020;16(1):60-68.
4. van der Heul HU, Bilyk BL, McDowall KJ, *et al.* Regulation of antibiotic production in Actinobacteria: New perspectives from the post-genomic era. Nat Prod Rep 2018;35(6):575-604.
5. Myronovskyi M, Luzhetskyy A. Native and engineered promoters in natural product discovery. Nat Prod Rep 2016;33(8):1006-1019.
6. Makitrynskyy R, Keller L, Kaur A, *et al.* Olikomycin A–A novel calcium-dependent lipopeptide with antibiotic activity against multidrug-resistant bacteria. Chem Eur J 2025;31(8):e202403985.
7. Brigham MW, Hems ES, Van DCL, *et al.* Discovery and biosynthesis of biffamycin A – a novel glycotetrapeptide antibiotic. bioRxiv [Preprint] 2025:2025.09.22.677794.
8. Xu XN, Chen LY, Chen C, *et al.* Genome mining of the marine actinomycete *Streptomyces* sp. DUT11 and discovery of tunicamycins as anti-complement agents. Front Microbiol 2018;9:1318.
9. Beniddir MA, Kang KB, Genta-Jouve G, *et al.* Advances in decomposing complex metabolite mixtures using substructure- and network-based computational metabolomics approaches. Nat Prod Rep 2021;38(11):1967-1993.
10. Hannigan GD, Prihoda D, Palicka A, *et al.* A deep learning genome-mining strategy for biosynthetic gene cluster prediction. Nucleic Acids Res 2019;47(18):e110.
11. Terlouw BR, Huang C, Meijer D, *et al.* PARAS: High-accuracy machine learning of substrate specificities in nonribosomal peptide synthetases. JACS Au 2026;6(4):2315-2336.
12. Blin K, Shaw S, Augustijn HE, *et al.* antiSMASH 7.0: New and improved predictions for detection, regulation, chemical structures and visualisation. Nucleic Acids Res 2023;51(W1):W46-W50.
13. Mózsik L, Hoekzema M, de Kok NAW, *et al.* CRISPR-based transcriptional activation tool for silent genes in filamentous fungi. Sci Rep 2021;11(1):1118.
14. Zhang MM, Wong FT, Wang Y, *et al.* CRISPR-Cas9 strategy for activation of silent *Streptomyces* biosynthetic gene clusters. Nat Chem Biol 2017;13(6):607-609.
15. Zhang F, Zhang F, Yu X, *et al.* Discovery of a novel family of Gram-negative-active cationic cyclolipopeptides by motif search-guided chemical synthesis. CCS Chem 2025;7(8):2442-2450.
16. Wang M, Carver JJ, Phelan VV, *et al.* Sharing and community curation of mass spectrometry data with Global Natural Products Social Molecular Networking. Nat Biotechnol 2016;34(8):828-837.
17. Nothias LF, Petras D, Schmid R, *et al.* Feature-based molecular networking in the GNPS analysis environment. Nat Methods 2020;17(9):905-908.
18. Chauvin IM, Davis LJ, Krunic A, *et al.* Discovery of suomilide and cyanopeptolin analogues by 15N stable isotope labeling and genome mining of cyanobacteria. J Nat Prod 2026;89(2):573-583.

19. Monge-Loría M, Brady C, Wu H, *et al.* Discovery of metallophore diversity in *Microbulbifer* in mixed culture with a coral pathogen using computational mass spectrometry and genome mining. bioRxiv [Preprint] 2026:2026.03.11.711190.
20. Asamizu S, Pramana AAC, Kawai SJ, *et al.* Comparative metabolomics reveals a bifunctional antibacterial conjugate from combined culture of *Streptomyces hygroscopicus* HOK021 and *Tsukamurella pulmonis* TP-B0596. ACS Chem Biol 2022;17(9):2664-2672.
21. Deng Q, Li Y, He W, *et al.* A polyene macrolide targeting phospholipids in the fungal cell membrane. Nature 2025;640(8059):743-751.
22. da Hora GCA, Oh M, Mifflin MC, *et al.* Lasso peptides: Exploring the folding landscape of nature's smallest interlocked motifs. J Am Chem Soc 2024;146(7):4444-4454.
23. Al Musaimi O. Lasso peptides realm: Insights and applications. Peptides 2024;182:171317.
24. Kadjo AE, Eustáquio AS. Bacterial natural product discovery by heterologous expression. J Ind Microbiol Biotechnol 2023;50(1):kuad044.
25. Ouyang X, Ran X, Zhu D, Yang ZJ. Predicting lasso peptide structure with LassoPred. Methods Enzymol 2026;730:91-106.
26. Jangra M, Travin DY, Aleksandrova EV, *et al.* A broad-spectrum lasso peptide antibiotic targeting the bacterial ribosome. Nature 2025;640(8060):1022-1030.
27. Jangra M, Travin DY, Aleksandrova EV, *et al.* Author correction: A broad-spectrum lasso peptide antibiotic targeting the bacterial ribosome. Nature 2025;645(8082):E11.
28. Silver LL. Lasso-shaped molecule is a new type of broad-spectrum antibiotic. Nature 2025;640(8060):887-889.
29. Jangra M, Travin DY, Kaur M, *et al.* An acetyltransferase conferring self-resistance of the producer to lasso peptide antibiotic lariocidin. ACS Infect Dis 2026;12(2):714-723.
30. Um S, Jeong H, Ganley JG, *et al.* Cebulassopins, antiproliferative lasso peptides from a split biosynthetic operon. J Am Chem Soc 2026;148(7):6739-6743.
31. Wen Y, Li Z, Ye J, *et al.* Discovery and characterization of actinosynnelassin: An anti-*Pseudomonas fluorescens* lasso peptide derived from a large precursor open reading frame. J Nat Prod 2025;88(6):1388-1398.
32. Negri T, Vitale GA, Adamek M, *et al.* Discovery and heterologous expression of the soil metagenome-derived lasso peptide metanodin with an unprecedented ring structure. J Nat Prod 2025;88(11):2625-2634.
33. Santos-Fernandez M, Jeanne Dit Fouque K, Karki U, *et al.* Structural landscape of syanodin I lasso peptide. Biochemistry 2026;65(9):1455-1464.
34. Fu Y, Pateri E, Kuipers OP. Discovery, biosynthesis, and characterization of rodencin, a two-component lanthipeptide, harboring D-amino acids introduced by the unusual dehydrogenase RodJA. J Nat Prod 2024;87(10):2344-2354.
35. Kaweewan I, Ijichi S, Nakagawa H, Kodani S. Heterologous production of new lanthipeptides hazakensins A and B using a cryptic gene cluster of the thermophilic bacterium *Thermosporothrix hazakensis*. World J Microbiol Biotechnol 2023;39(1):30.
36. Roblero-Mejía DO, García-Ausencio C, Rodríguez-Sanoja R, *et al.* Embleporicin: A novel class I lanthipeptide from the Actinobacteria *Embleya* sp. NF3. Antibiotics (Basel) 2024;13(12):1179.
37. Liu Z, Li H, Yu Q, *et al.* Heterologous expression facilitates the production and characterization of a class III lanthipeptide with coupled labionin cross-links in sponge-associated *Streptomyces rochei* MB037. ACS Chem Biol 2024;19(9):2060-2069.
38. Rukthanapitak P, Saito K, Kobayashi R, *et al.* Heterologous production of a new lanthipeptide boletupeptin using a cryptic biosynthetic gene cluster of the myxobacterium *Melittangium boletus*. J Biosci Bioeng 2024;137(5):354-359.
39. Choi B, Link AJ. Discovery, function, and engineering of graspetides. Trends Chem 2023;5(8):620-633.
40. Choi B, Acuña A, Link AJ. Cyclic peptides from graspetide biosynthesis and native chemical ligation. J Am Chem Soc 2024;146(17):11605-11609.
41. Carter RS, Ramesh S, Saad H, *et al.* Discovery of partner protein-dependent graspetide biosynthesis. ACS Chem Biol 2026;21(4):698-709.
42. Choi B, Johnson TG, Acuña A, *et al.* Peptide and protein cyclization by a promiscuous graspetide synthetase. ACS Cent Sci 2025;11(7):1111-1121.
43. Rubin GM, Patel KP, Jiang Y, *et al.* Characterization of a dual function peptide cyclase in graspetide biosynthesis. ACS Chem Biol 2024;19(12):2525-2534.
44. Choi B, Acuña A, Koos JD, Link AJ. Large-scale bioinformatic study of graspimiditides and structural characterization of albusimiditide. ACS Chem Biol 2023;18(11):2394-2404.
45. Arnison PG, Bibb MJ, Bierbaum G, *et al.* Ribosomally synthesized and post-translationally modified peptide natural products: Overview and recommendations for a universal nomenclature. Nat Prod Rep 2013;30(1):108-160.
46. Saha S, Zhang Y, Cheng Y, Ting CP. Evolution of a strategy for the unified synthesis of enteropeptin sactipeptides. J Org Chem 2026;91(9):3529-3544.
47. Shamseddine L, Roblin C, Veyrier I, *et al.* Mechanistic and functional aspects of the Ruminococcin C sactipeptide isoforms. isci 2023;26(9):107563.

48. Elsakhawy OK, Abouelkhair MA. Genome mining reveals a sactipeptide biosynthetic cluster in *Staphylococcus pseudintermedius*. Vet Sci 2025;12(7):635.
49. Jia Y, Han Y, Wang W, *et al.* Production of subtilosin A in *E. coli*: Insights into the head-to-tail macrocyclization. Org Biomol Chem 2025;23(28):6694-6698.
50. Ruíz-De-Anda D, Mendoza-Acosta MF, Casados-Vázquez LE. Exploring thurincin H as a biotechnologically relevant sactipeptide after fifteen years of research. Arch Microbiol 2025;207(8):171.
51. Juárez-Cortés MZ, Casados Vázquez LE, Rivera Camacho AR, *et al.* Characterization and potential application of thurincin H as an alternative to antibiotics in the control of *Streptococcus iniae*. J Invertebr Pathol 2026;216:108550.
52. Machushynets NV, Elsayed SS, Du C, *et al.* Paenitracins, a novel family of bacitracin-type nonribosomal peptide antibiotics produced by plant-associated *Paenibacillus* species. mSystems 2026;11(3):e0149625.
53. Renard S, Versluys S, Taillier T, *et al.* Optimization of the antibacterial spectrum and the developability profile of the novel-class natural product corramycin. J Med Chem 2023;66(24):16869-16887.
54. Adam S, Fries F, von Tesmar A, *et al.* The peptide antibiotic corramycin adopts a β-hairpin-like structure and is inactivated by the kinase ComG. J Am Chem Soc 2024;146(13):8981-8990.
55. Siebert A, Kazmaier U. Chemical ligation-mediated total synthesis of corramycin. Org Lett 2024;26(15):3169-3173.
56. Fenwick MK, Pierce PG, Abendroth J, *et al.* Exquisite selectivity of griselimycin extends to the beta subunit of DNA polymerases from Gram-negative bacterial pathogens. Commun Biol 2024;7(1):1622.
57. Kling A, Lukat P, Almeida DV, *et al.* Targeting DnaN for tuberculosis therapy using novel griselimycins. Science 2015;348(6239):1106-1112.
58. Spira A, Dash R, Lepori I, *et al.* Molecular determinants governing the antitubercular activity of griselimycin. bioRxiv [Preprint] 2026:2026.03.19.712639.
59. Crocoll S, Götz S, Munz L, *et al.* BPS2026 – Cyclic lipopeptides (CLiPs)-membrane interactions: Insights into membrane binding and permeabilization. Biophys J 2026;125(4):350a.
60. Ait Assou S, El Hassouni M. New *Streptomyces*-derived antibacterial compounds targeting Gram-positive bacteria: A systematic review. ScientificWorldJournal 2025;2025:6659874.
61. Xie TP, Yi MZ, Duan R, *et al.* The discovery of nocacyclomycins A-H, cyclic lipodepsipeptides from *Nocardia sungurluensis* YINM00009. J Nat Prod 2026;89(1):115-127.
62. Ortiz-López FJ, Oves-Costales D, Guerrero Garzón JF, *et al.* Genome-led discovery of the antibacterial cyclic lipopeptide kutzneridine A and its silent biosynthetic gene cluster from *Kutzneria* species. J Nat Prod 2024;87(10):2515-2522.
63. Fernández-Pastor I, Ortiz-López FJ, Oves-Costales D, *et al.* Dilarmycins A-C, calcium-dependent lipopeptide antibiotics with a non-canonical $Ca^{2+}$-binding motif. Org Lett 2024;26(7):1343-1347.
64. Gong B, Bai E, Feng X, *et al.* Characterization of chalkophomycin, a copper(II) metallophore with an unprecedented molecular architecture. J Am Chem Soc 2021;143(49):20579-20584.
65. Crooke AM, Chand AK, Cui Z, *et al.* Elucidation of chalkophomycin biosynthesis reveals N-hydroxypyrrole-forming enzymes. J Am Chem Soc 2024;146(23):16268-16280.
66. Kim JW, Shin-ya K, Furihata K, *et al.* Oximidines I and II: Novel antitumor macrolides from *Pseudomonas* sp. J Org Chem 1999;64(1):153-155.
67. Vriens E, De Ruysscher D, Weir ANM, *et al.* Polyketide synthase-mediated O-methyloxime formation in the biosynthesis of the oximidine anticancer agents. Angew Chem Int Ed Engl 2023;62(34):e202304476.
68. Hartkoorn RC, Sala C, Neres J, *et al.* Towards a new tuberculosis drug: Pyridomycin - nature's isoniazid. EMBO Mol Med 2012;4(10):1032-1042.
69. Lee B, Hwang GJ, Jang JP, *et al.* Discovery of pyridomycin derivatives as InhA inhibitors from actinomycetes through molecular networking and an in-house tandem mass library. Nat Prod Bioprospect 2026;16(1):25.
70. Du H, Zhou Z, Han S, *et al.* Biosynthesis of the L-pyridylalanine moiety in antimycobacterial pyridomycin via a PKS-NRPS hybrid system. Org Lett 2026;28(9):2971-2976.
71. Valderrama K, Horlacher O, Publicola G, *et al.* Optimizing the antibiotic potency and metabolic stability of pyridomycin using a semisynthetic approach. J Med Chem 2026;69(3):2496-2508.
72. Bhattarai K, Majer T, Haussmann M, *et al.* Salamandamide lipodipeptides are biosynthetic intermediate shunt products of the nonmodular nonribosomal peptide assembly lines of the viscosin family. J Nat Prod 2025;88(4):1012-1022.
73. Fries F, Walesch S, Jansen R, *et al.* Structure elucidation, biosynthesis and biological evaluation of neosorangicin A, a member of the sorangicin family. J Nat Prod 2026;89(4):1226-1237.
74. Zeng H, Birkelbach J, Hoffmann J, *et al.* Expanding the ajudazol cytotoxin scaffold: Insights from genome mining, biosynthetic investigations, and novel derivatives. J Nat Prod 2022;85(11):2610-2619.
75. Xing C, Yang H, Lv K, *et al.* Genome mining and heterologous expression-guided discovery of mangicol sesterterpenoids with antimicrobial and antineuroinflammatory activities. J Agric Food Chem 2025;73(31):19474-19483.

76. Holland DC, Iizumi R, Shende VV, *et al.* Isolation of verrucosins A-E from a marine *Verrucosispora* sp. reveals a unifying biosynthetic hypothesis for linear and macrocyclic polyketides. J Nat Prod 2025;88(7):1631-1642.
77. Zhao M, Zhang W, Yang C, *et al.* Discovery of kebanmycins with antibacterial and cytotoxic activities from the mangrove-derived *Streptomyces* sp. SCSIO 40068. J Nat Prod 2024;87(6):1591-1600.
78. Wang Y, Zhou L, Pan X, *et al.* Metabolic blockade-based genome mining of sea anemone-associated *Streptomyces* sp. S1502 identifies atypical angucyclines WS-5995 A-E: Isolation, identification, biosynthetic investigation, and bioactivities. Mar Drugs 2024;22(5):195.
79. Ma Z, Huang Z, Liao Y, *et al.* Deciphering the δ-lactam formation and iron-reducing activity of spinactins from *Saccharopolyspora spinosa*. Org Lett 2025;27(2):565-570.
80. Rojas-Villalta D, Núñez-Montero K, Chavarría-Pizarro L. Social wasp-associated *Tsukamurella* sp. strains showed promising biosynthetic and bioactive potential for discovery of novel compounds. Sci Rep 2024;14(1):21118.
81. Tistechok S, Bratiichuk D, Sucipto H, *et al.* Gromomycins: An unprecedented class of triterpene antibiotics produced by a novel biosynthetic pathway. Angew Chem Int Ed Engl 2025;64(22):e202422270.
82. Chaudhri AA, Kakumu Y, Thiengmag S, *et al.* Functional redundancy and dual function of a hypothetical protein in the biosynthesis of eunicellane-type diterpenoids. ACS Chem Biol 2024;19(11):2314-2322.
83. Shen L, Wang Y, Liu C, *et al.* Genome-driven discovery of antiviral atralabdans A-C from the soil-dwelling *Streptomyces atratus*. J Nat Prod 2024;87(7):1735-1745.
84. Park C, Tsutsumi S, Mitsuhashi T, *et al.* Discovery of a new type of terpene synthase coded by an orphan gene in a giant virus. Biochemistry 2025;64(18):3866-3871.
85. Li XY, Lv JM, Cao ZQ, *et al.* Biosynthetic characterization of the antifungal fernane-type triterpenoid polytolypin for generation of new analogues via combinatorial biosynthesis. Org Biomol Chem 2023;21(4):851-857.
86. Falcao BP, Di Matteo V, Hrouzek P, *et al.* Cyanochelin B: A cyanobacterium-produced siderophore with photolytic properties that negate iron monopolization in UV light. Appl Environ Microbiol 2025;91(11):e0256624.
87. Sousa ML, Ferreira L, Ferreira D, *et al.* Decoding lusichelins A-E: An in-depth look at the metallophores of *Lusitaniella coriacea* LEGE 07167: Structure, production, and functionality. J Nat Prod 2025;88(6):1319-1333.
88. Cha L, Qian C, Padhi C, *et al.* Discovery and biosynthesis of nitrilobacillins by post-translational introduction of C-terminal nitrile groups. J Am Chem Soc 2026;148(26):27430-27441.
89. Kralova S, Spacek P, Gafriller J, *et al.* Kineochelins: A novel group of siderophores from an Antarctic bacterium. bioRxiv [Preprint] 2026:2026.02.23.707395.
90. Leprevost L, Jünger S, Lippens G, *et al.* A widespread family of ribosomal peptide metallophores involved in bacterial adaptation to metal stress. Proc Natl Acad Sci U S A 2024;121(49):e2408304121.
91. Lippens G, Li Y, Jacob-Dubuisson F, Dubiley S. Selective labeling supports 5-thiooxazole post-translational modification in bufferins. bioRxiv [Preprint] 2025:2025.12.15.693703.
92. Xue D, Wu Q, Hou L, *et al.* Discovery and biosynthetic interrogation of a cobalt-containing terpene-polyketide-nonribosomal peptide tribrid with anticoronavirus activity. J Am Chem Soc 2025;147(42):38951-38957.
93. Zytnick AM, Gutenthaler-Tietze SM, Aron AT, *et al.* Identification and characterization of a small-molecule metallophore involved in lanthanide metabolism. Proc Natl Acad Sci U S A 2024;121(32):e2322096121.
94. Gutenthaler-Tietze SM, Mertens M, Phi MT, *et al.* Comparative binding studies of the chelators methylolanthanin and rhodopetrobactin B to lanthanides and ferric iron. ChemBioChem 2026;27(1):e202500312.
95. Castelo-Branco R, Pereira JP, Freitas S, *et al.* Genome-informed discovery of monchicamides A-K: Cyanobactins from the Microcoleaceae cyanobacterium LEGE 16532. J Nat Prod 2025;88(1):86-93.
96. Brito Â, Martins T, Freitas S, *et al.* Isolation and biosynthesis of hyellamide, a glycosylated N-acyltyrosine derivative, from the cyanobacterium *Hyella patelloides* LEGE 07179. J Nat Prod 2025;88(3):850-856.
97. Alexander KL, Naman CB, Iwasaki A, *et al.* Fatuamide A, a hybrid PKS/NRPS metallophore from a *Leptolyngbya* sp. marine cyanobacterium collected in American Samoa. J Nat Prod 2025;88(2):322-335.
98. Adak S, Chase AB, Skrip AE, *et al.* Metagenomic identification of brominated indole biosynthetic machinery from cyanobacteria. J Nat Prod 2025;88(7):1734-1742.
99. Salmaso N, Cerasino L, Pindo M, *et al.* Taxonomic and functional metagenomic assessment of a *Dolichospermum* bloom in a large and deep lake south of the Alps. FEMS Microbiol Ecol 2024;100(10):fiae117.
100. Zhou Z, Yang J, Ma J, *et al.* Antarmycins: Discovery, biosynthesis, anti-pathogenic bacterial activity, and mechanism of action from deep-sea-derived *Pseudonocardia antarctica*. JACS Au 2025;5(1):237-249.
101. Ragozzino C, Palma Esposito F, Buonocore C, *et al.* Integrated genome and metabolome mining unveiled structure and biosynthesis of novel lipopeptides from a deep-sea *Rhodococcus*. Microb Biotechnol 2024;17(11):e70011.
102. Chen L, Liu K, Hong J, *et al.* The discovery of weddellamycin, a tricyclic polyene macrolactam antibiotic from an Antarctic deep-sea-derived *Streptomyces* sp. DSS69, by heterologous expression. Mar Drugs 2024;22(4):189.
103. Kumar P, Nalli Y, Singh S, *et al.* Dactylides D and E, two modified 22-membered polyol macrolides isolated from *Dactylosporangium aurantiacum*. J Antibiot (Tokyo) 2026;79(6):415-418.
104. Bahadoor A, Brauer EK, Bosnich W, *et al.* Gramillin A and B: Cyclic lipopeptides identified as the nonribosomal biosynthetic products of *Fusarium graminearum*. J Am Chem Soc 2018;140(48):16783-16791.

105. Brauer EK, Bosnich W, Holy K, *et al.* A cyclic lipopeptide from *Fusarium graminearum* targets plant membranes to promote virulence. Cell Rep 2024;43(7):114384.
106. Nie Q, Zhao F, Yu X, *et al.* A class of benzofuranoindoline-bearing heptacyclic fungal RiPPs with anticancer activities. Nat Chem Biol 2025;21(12):1938-1947.
107. Witte TE, Harris LJ, Paquette LA, *et al.* Discovery of fusadapamides, accessory chromosome-associated metabolites incorporating L-2,3-diaminopropionic acid in *Fusarium poae*. J Nat Prod 2025;88(12):2883-2896.
108. Meng LH, Awakawa T, Li XM, *et al.* Discovery of (±)-penindolenes reveals an unusual indole ring cleavage pathway catalyzed by P450 monooxygenase. Angew Chem Int Ed Engl 2024;63(26):e202403963.
109. Avalon NE, Reis MA, Thornburg CC, *et al.* Leptochelins A-C, cytotoxic metallophores produced by geographically dispersed *Leptothoe* strains of marine cyanobacteria. J Am Chem Soc 2024;146(27):18626-18638.